Research Square

Preprints are preliminary reports that have not undergone peer review.
They should not be considered conclusive, used to inform clinical practice,
or referenced by the media as validated information.

A non-redundant role of OsGELP87 in lipid-associated pollen development and fertility in rice

Kayyis Muayadah Lubba
Hokkaido University
Yuji Kishima
kishima@agr.hokudai.ac.jp

Hokkaido University

Research Article

Keywords: Rice (Oryza sativa), OsGELP87, pollen development, male fertility, lipid metabolism, crop resilience

Posted Date: March 16th, 2026

DOI: https://doi.org/10.21203/rs.3.rs-9079152/v1

License: This work is licensed under a Creative Commons Attribution 4.0 International License. Read Full License

Additional Declarations: No competing interests reported.

A non-redundant role of OsGELP87 in lipid-associated pollen development and fertility in rice.

Kayyis Muayadah Lubba[1], Yuji Kishima [2*]

[1]Graduate School of Agriculture, Hokkaido University, Sapporo 060-8589, Japan

[2]Research Faculty of Agriculture, Hokkaido University, Sapporo 060-8589, Japan

***Corresponding author**

Yuji Kishima: Research Faculty of Agriculture, Hokkaido University, Sapporo 060-8589, Japan. kishima@agr.hokudai.ac.jp

Kayyis Muayadah Lubba: ORCID 0009-0002-0094-5568

Yuji Kishima: ORCID 0000-0002-0942-3371

ABSTRACT (198 words)

Pollen fertility in flowering plants relies on precise lipid metabolism, yet the enzymatic regulators underlying these processes remain incompletely understood. Here we identify OsGELP87, a GDSL-type esterase/lipase, as a key regulator of male gametophyte development in rice (*Oryza sativa*). Phylogenetic analysis revealed that OsGELP87 lacks closely related paralogs, suggesting limited functional redundancy. CRISPR–Cas9 genome editing revealed impaired pollen wall architecture, abnormal nuclear morphology, and reduced lipid droplet accumulation, causing reduced male fertility. Complete loss-of-function mutants were not recovered. Transcriptome and qRT–PCR analyses revealed disrupted lipid metabolic networks, including suppression of FAD2 and pollen lipid transfer proteins, together with altered redox regulators. Structural modelling showed that a premature stop codon in exon 3 abolishes conserved C-terminal motifs and predicted palmitoylation sites, likely impairing catalytic function. Functional analyses suggest that OsGELP87 participates in sporopollenin/tryphine assembly during pollen wall formation and triacylglycerol mobilization during pollen germination. Population genomic analysis uncovered five haplotypes with distinct geographic distributions and fertility phenotypes, while no haplotypes carrying non-

functional alleles were detected. Together, these results identify OsGELP87 as a non-redundant regulator of lipid-associated cellular processes required for pollen development and provide new insight into how lipid metabolism contributes to reproductive cell differentiation in plants.

KEYWORDS

Rice (*Oryza sativa*); OsGELP87; pollen development; male fertility; lipid metabolism; crop resilience

KEY MESSAGE (29 words)

OsGELP87 is non-redundant component of a lipid processing network required for pollen maturation. The absence of loss-of-function *OsGELP87* highlights its evolutionary constraint and underscores the importance in reproductive success.

ACKNOWLEDGEMENTS (43 words)

We would like to express our sincere gratitude to Dr. Koichi Yamamori and Dr Yohei Koide for their invaluable assistance and insightful suggestions.

INTRODUCTION (743 words)

Pollen development in rice (*Oryza sativa*) relies on the coordinated formation of a robust wall composed of an inner intine and an outer exine (Zhang et al., 2022). The exine, derived from tapetum-supplied precursors, is rich in sporopollenin and lipidic compounds that provide structural integrity and protect developing pollen (Quilichini et al., 2015; Zhou et al., 2025).

Lipids play multiple essential roles in pollen development: they are structural components of the exine and pollen coat, facilitate proper sporopollenin deposition, maintain membrane fluidity, and serve as energy reserves during pollen germination and tube growth. Disruption in lipid metabolism can lead to defective exine assembly, compromised pollen coat formation, and reduced fertility. Several lipid-related genes in rice, including *OsC6*, *OsGPAT3*, *OsDGD1*, and *OsFAD2*, are critical for pollen wall formation, highlighting the central importance of lipid synthesis, mobilization, and remodelling in ensuring pollen viability (Zhang et al., 2020).

There are many gene family related to lipids, among which GDSL esterases/lipases (GELPs) are a particularly important family, which are a large and multifunctional subgroup of plant lipases, defined by a conserved Ser–Gly–Asn–His catalytic motif (Shen et al., 2022). They participate in pollen exine formation, cuticle biosynthesis, cell wall modification, lipid metabolism, and stress responses (Chepyshko et al., 2012; Shen et al., 2022). Another feature of GELP is that it is secreted into the extracellular space (the apoplast) via a signal peptide (Shen et al., 2022; Rastogi et al., 2022). This enables it to catalyse the insoluble lipids present in cell walls and outer layers directly. (Xu et al., 2014). Many GELPs are co-expressed with the gene families responsible for the oxidative stress response (ROS control) and the defense response (Duan et al., 2023). Fatty acids and lysophosphatidic acid (LPA), which are generated through the hydrolysis of lipids, act as secondary messengers that activate hormone pathways such as those for jasmonic acid (JA), salicylic acid (SA) and abscisic acid (ABA). GELPs initiate a chain reaction involving stress sensing, lipid modification, signal generation and gene response, forming the common foundation underlying multifaceted

phenomena such as the maintenance of pollen fertility, cold adaptation and defense responses.

Although 115 *GELP* genes are annotated in rice, only a few have been functionally characterized: *OsGELP110* and *OsGELP115* for pollen exine formation, *OsGELP33* and *OsGELP62* in cell wall biosynthesis, *OsGELP34* in lipid homeostasis, *OsGELP112*/*WDL1* in water regulation, and *OsGLIP1* and *OsGLIP2*/*OsGELP78* in disease resistance (Park et al., 2010; Gao et al., 2017; Zhang et al., 2017, 2019, 2020; Yuan et al., 2020; He et al., 2021; Lubba et al., 2025). The majority of GELPs remain uncharacterized, and their roles in rice pollen development are largely unknown.

Recent transcriptomic analyses of cold-tolerant rice cultivars have shown that several GELP genes maintain stable expression in anthers even under low temperature (Yamamori et al., 2025). *OsGELP87* exhibits the strongest and most specific expression during the booting stage—when lipid accumulation and pollen wall formation occur—suggesting a key role in reproductive lipid remodelling. Considering the established sensitivity of anther development to cold stress and the potential link between lipid dynamics and fertility maintenance, *OsGELP87* was selected as a prime candidate to investigate how lipid-modifying enzymes contribute to pollen viability under environmental constraints.

We compared the expression profiles of all 115 *OsGELP* genes across rice tissues (Lubba et al. 2025). Among the *OsGELP* family members, *OsGELP87* showed high expression in anthers at the booting stage (Yamamori et al. 2025 and **Fig. S1**). *OsGELP87* showed preferential and elevated expression in anthers, strongly suggesting a reproductive role (Yamamori et al. 2025). Based on amino acid sequence prediction, *OsGELP87* is predicted to be a secreted protein that undergoes palmitoylation and functions across both membranes and the extracellular matrix. This makes it unique in terms of intracellular metabolism. There is no alternative gene involved in pollen development and no analysis of natural mutants has yet been reported. Together, these facts suggest that *OsGELP87* plays a unique and irreplaceable role in pollen development.

Here, we focus on *OsGELP87* to elucidate its molecular and physiological roles in rice anther development. By integrating CRISPR/Cas9-mediated mutagenesis, transcriptomic profiling, and population genomic analysis, we demonstrate that *OsGELP87* plays a significant role in pollen fertility. It is likely to function as a key component of lipid metabolic networks that coordinates pollen wall formation and redox regulation —offering new insights into the lipid-based regulation of gametophyte development and its evolutionary adaptation to diverse environments.

RESULT (2923 words)

***OsGELP87* is a primary anther-expressed GELP gene**

Integrated analysis of transcriptomic datasets identified *OsGELP87* as the most prominently anther-enriched GDSL esterase/lipase (GELP) gene in rice, providing strong evidence for its role in pollen development (**Fig. S1**). Analysis of the RiceXPro database showed that *OsGELP87* exhibited on of the highest normalized expression (z-score) across four anther developmental stages, whereas most other GELP family members displayed minimal or negligible expression (**Fig. S1a**). Re-analysis of microarray and RNA-seq transcriptomic datasets extracted from Yamamori *et al.* (2025) demonstrated that *OsGELP87* ranked among the top-expressed GELP genes during the booting stage across multiple rice cultivars, indicating a conserved expression pattern independent of genetic background (**Fig. S1b, S1c, and S2a)**. RNA-seq analysis revealed that *OsGELP87* transcript was one of highest accumulations in anthers of four distinct rice varieties (**Fig. S1c**). Importantly, qRT-PCR analysis across major vegetative and reproductive organs confirmed that *OsGELP87* expression was strongly enriched in anthers compared with leaves, stems, and roots, validating the transcriptomic findings (**Fig. S2b)**. These multiple transcriptional data experimentally suggest, together, that *OsGELP87* functions primarily as an anther GELP gene, playing an essential role in pollen development.

Structural conservation of *OsGELP87*

A total of 114 GDSL lipase/esterase genes have been annotated in the rice genome, designated *OsGELP1* to *OsGELP114* (Chepyshko et al., 2012, RAB-DP, https://rapdb.dna.affrc.go.jp/). Among them, LOC_Os06g0636700 corresponds to *OsGELP87*. The *OsGELP87* protein comprises 382 amino acids, including a 30–amino acid N-terminal signal peptide and a conserved GDSL-lipase domain (**Fig.1a**). Signal peptide (Sec/SPI) prediction using SignalP 6.0 yielded a high probability score of 0.9598, indicating that *OsGELP87* is most likely involved in the secretory pathway (**Fig.1a**). To further assess potential lipid modifications and localization, we performed in silico predicting analyses. GPS-Lipid web-based software (http://www.lipid.biocuckoo.org/) predicted two high-confidence S-palmitoylation sites at Cys267 and Cys376, suggesting that *OsGELP87* may undergo dynamic membrane anchoring (**Fig. S3**). WoLF PSORT, Plant-mPLoc, and DeepLoc web-based softwares predicted extracellular or secretory localization (**Fig. S3**), and SignalP 6.0 (https://services.healthtech.dtu.dk/services/SignalP-6.0/) confirmed a strong signal peptide cleavage site between residues 30 and 31 (**Fig. S3**). These results indicate that *OsGELP87* is a secretory protein whose membrane association may be regulated by palmitoylation.

Phylogenetic relationships of *OsGELP87* with the other related genes

Phylogenetic analysis places *OsGELP87* clusters most closely with *OsGELP32* (Chepsyco et al., 2012), together with *OsGELP31*, *OsGELP97*, *OsGELP98*, and *OsGELP99*, supported by high bootstrap values (≥88–100), reflecting strong evolutionary conservation (**Fig. 1b**). Consistent with their close phylogenetic relationship, *OsGELP87* and *OsGELP32* share high amino acid similarity (80% amino acid), including a conserved GDSL lipase domain, catalytic motifs, and an N-terminal signal peptide, indicating comparable enzymatic potential and secretory targeting (**Fig. S4a and S4b**). Despite this strong structural conservation, their expression patterns have markedly diverged: *OsGELP87* shows strong and preferential expression in reproductive tissues (**Fig. S4c**), particularly anthers and panicles, whereas *OsGELP32* exhibits broader expression with enrichment in the ovary and minimal expression in anthers (**Fig. S4c**).

To gain insight into the potential function of *OsGELP87*, we performed phylogenetic analysis with GDSL family members from rice and other plant species with reported functional characterization. *OsGELP87* was found to be most closely related to *Arabidopsis thaliana AtEXL4* (**Fig. 1**). Notably, *AtEXL* family genes (*AtEXL4*, *AtEXL5*, and *AtEXL6*) are directly regulated by the transcription factor *Aborted microspore* (*AMS*), which is essential for anther development (Xu et al., 2010). *AtEXL5* and *AtEXL6* are expressed in the tapetum and localized in the tapetum and pollen coat, whereas *AtEXL4* expression is highly specific to anthers but undetectable in microspores (Xu et al., 2014). Similarly, *OsGELP87* clustered within the same clade as several rice GELPs previously reported to be highly expressed in anthers, including *OsGELP58*, *OsGELP56*, *OsGELP34*, *OsGELP110*, and *OsGELP115* **(Fig.1b)** (Chepyshko et al., 2012 and Lubba et al., 2025). Among them, *OsGELP34*, *OsGELP110*, and *OsGELP115* have been implicated in lipid homeostasis and pollen fertility (Deng et al., 2020).

Haplotype diversity with adaptation of *OsGELP87* but non-null Haplotype

The *OsGELP87* gene is located on chromosome 6 (chr06:25,870,258–25,876,328; 6,070 bp, minus strand, RABDP database). Single nucleotide polymorphisms (SNPs) were distributed across both coding and non-coding regions (**Fig. 2a**). Although some SNPs are present in exons, we failed to identify any null haplotypes in the 3K rice genome dataset**,** implicating that *OsGELP87* is not redundant in the rice genome (**Fig. 2a**). Haplotype analysis of *OsGELP87* across the 3K rice dataset uncovered five major haplotypes with distinct patterns of distribution and functional divergence (**Fig. 2a**). Sequence analysis of the **OsGELP87** promoter region revealed nucleotide polymorphisms at positions 13 and 16 upstream of the promoter (**Fig. S5a**). However, these promoter-site differences do not distinguish **Hap.1** and **Hap.4**, which differ only by a single SNP in the CDS, suggesting that haplotype-specific regulation of **OsGELP87** expression is unlikely to be driven by promoter variation (**Fig. S5a, b**). Hap.2, Hap.3, and Hap.4 emerged as predominant haplotypes, particularly enriched in indica subgroups, whereas Hap.1 and Hap.5 were rare and confined to specific subpopulations (**Fig. 2b and 2c**). Latitude-based comparisons revealed strong geographic stratification, with Hap.1 occurring at high latitudes with high pollen fertility (**Fig. S5c**), in contrast to the broader distribution of Hap.2-4 across tropical and

subtropical regions, with lower pollen fertility (**Fig. 2b; S5c; S5d**). Network analysis positioned Hap.2 and Hap.4 as main haplotypes with high accession numbers, suggesting they represent core alleles selected during rice domestication and expansion (**Fig. 2c**). Geographic mapping further demonstrated that *OsGELP87* haplotypes are unevenly distributed across Asia, Africa, and tropical ecosystems, reflecting both demographic history and local ecological adaptation (**Fig. 2d**). These results highlight *OsGELP87* as a domestication and adaptation-linked gene whose allelic diversity underlies ecological specialization in rice.

The alignment reveals that all *OsGELP87* haplotypes share a highly conserved structure, including the signal peptide and multiple GDSL lipase motifs, suggesting a preserved functional role across haplotypes (**Fig. S6**). The catalytic serine residue (S-Pamitolayton site, shown in magenta) is strictly conserved, indicating that the enzymatic activity related to lipid hydrolysis or transfer is maintained. Minor amino acid variations outside the conserved domains may contribute to subtle functional or expression differences among haplotypes (**Fig. S6**). All *OsGELP87* haplotypes display a similar overall fold, indicating functional conservation of the GDSL lipase domain (**Fig. S7**). However, amino acid substitutions at residues 34 and 56 alter the physicochemical environment near the catalytic residue Arg258 (**Fig. S7**). In Hap.1 and Hap.2/Hap.3/Hap.4 (wild type: WT), Glu34–Ala56–Arg258 interactions are predicted to stabilize the catalytic core, consistent with normal enzymatic activity (**Fig. S7a and S7b**). In contrast, Hap.5 carries Glu→Gly and Ala→Elo substitutions at positions 34 and 56, respectively, which disrupt hydrogen bonding (**Fig. S7c**). Although these conformational variations may underlie functional divergence among *OsGELP87* haplotypes, no non-functional haplotypes have been detected (**Fig. S7**).

CRISPR/Cas9 alters *OsGELP87* gene

No null allele of *OsGELP87* has been identified in natural rice populations, despite extensive sequence variation, suggesting strong selective constraint on this gene. To directly determine its biological role, the genome editing using CRISPR/Cas9 was performed targeting all exons of *OsGELP87* (exons 1, 2, and 3). Mutations were successfully obtained at all target sites except exon 1 (**Fig. 3, S8, and S9a**). The

genome-edited *OsGELP87* sequences are referred to as *'osgelp87'* hereafter. We have not yet obtained a homozygous, completely non-functional allele of exon 1. CRISPR–Cas9 targeting of exon 1 of *OsGELP87* yielded no regenerants, suggesting that severe disruption of *OsGELP87* function may impair cellular viability during regeneration, although alternative explanations such as technical constraints cannot be excluded. Two alleles carried mutations in exon 2: *osgelp87.2a* (1-bp deletion) and *osgelp87.2b* (1-bp insertion), while *osgelp87.3* contained a 1-bp insertion in exon 3 (**Fig. S9a**). We refer to these plants as genome-edited plants. This is because they reduce gene function, but not be knockout.

The wild type (WT) protein contains a complete signal peptide, four conserved GDSL motifs, and two predicted S-palmitoylation sites. It functions as a secreted lipid hydrolase. All genome-edited plants show varying degrees of C-terminal truncation and domain loss. In *osgelp87.2a*, the 1-bp deletion in exon 2 caused a frameshift (**Fig. S10a**), resulting in altered amino acid sequences and loss of conserved motifs, including multiple GDSL motifs and predicted palmitoylation sites (**Fig. S10b**). Structural modelling revealed major conformational changes, including the loss of five α-helices and one β-sheet, as well as the partial truncation of the signal peptide region. These changes impair protein stability (**Fig. S10c**). The *osgelp87.2b* plant carried a 1-bp insertion in exon 2 (**Fig. S11a**), which shifted the reading frame and eliminated conserved motifs within the catalytic region, including palmitoylation sites (**Fig. S11b**). Protein modelling revealed disruption of secondary structures, with loss of five α-helices, one β-sheet, and distortion of the signal peptide sequence (**Fig. S11c**). In *osgelp87.3*, the single-base insertion (+1 A) induced a frameshift that introduced a premature stop codon and caused the reduction of 2 alpha-helix compared to WT (**Fig. 3b, Fig. 3c**). The resulting truncated protein lacked the C-terminal region containing predicted S-palmitoylation motifs, which are essential for lipid modification and membrane anchoring (**Fig. S6**).

OsGELP87 is required for anther development and pollen fertility in rice

For phenotypic analyses, the edited lines possessed the following genome editing of *OsGELP87* alleles: *osgelp87.2a*, *osgelp87.2b*, and *osgelp87.3*. Due to the difficulty of

producing seeds with *osgelp87.2a*, *osgelp87.2*, and *osgelp87.3* was therefore mainly used for subsequent functional analyses. To investigate the phenotypic effects of *OsGELP87*, we compared the floral morphology and cytological characteristics of WT and *osgelp87.3* genome-edited plant, which carry a 1-bp adenine insertion in exon 3. Microscopic analysis revealed that WT anther is more yellow (**Fig. 4a**) pollen grains maintained a typical round shape, whereas *osgelp87.3* pollen grains were frequently collapsed and shrunken, indicative of defective pollen wall integrity (**Fig. 4b and S12a**). Consistently, I_2–KI staining and pollen viability demonstrated a strong reduction in both pollen fertility and viability in the genome-edited plant and quantitative analysis confirmed a reduction of more than half in *osgelp87.3* compared with WT (**Fig. 4c, 4d, and 4e**). Importantly, a similar reduction in pollen fertility was observed in the T_2 generation of **S12a**), confirming the stability of this phenotype. While sterile pollen grains showed no significant difference in diameter between WT and genome-edited plant, fertile pollen grains of *osgelp87.3* were slightly smaller, reflecting impaired pollen maturation (**Fig. 4F**). In the T2 generation, pollen size was significantly reduced in *osgelp87*.3, compared with WT (**Fig. S13c, d**), further supporting the essential role of *OsGELP87* in male fertility. Not only was pollen viability reduced, but the pollen tube length after germination and anther length was also shorter in the genome-edited plant compared with the WT (**Fig. 4g, 4h, S13d, S14**). Seed fertility in *osgelp87.2a, osgelp87.2b,* and *osgelp87.3* decreased significantly compared to WT, and a similar reduction appeared in pollen fertility, comparable to the *osgelp87.3* : WT ratio. Thus, the reduction may not be responsible for the female gamete, as its fertility is half of the WT line (**Fig. 4I, S13a, and S13b**). Despite the severe reduction in pollen fertility observed in *osgelp87.3* plants, the length of the stigma and pistil was not significantly different compared with WT plants (**Fig. 4h, S15a, b**). The genome-edited plants exhibited that plant height, flag leaf length, and heading date were largely unaffected (**Fig. S16a–c**). In addition, the kinetics of seed germination and the development of seedling were indistinguishable from those of WT (**Fig. S16d, e**). These results suggest that *OsGELP87* specifically influences pollen development and male fertility but does not affect pistil size or morphology.

Genome-edited *osgelp87* alters agronomic traits

To assess whether loss of *OsGELP87* affects agronomic performance, we compared key yield-related traits between WT and *osgelp87* genome-edited plant lines. The *osgelp87.3* exhibited a dramatic reduction in panicle number compared with WT (**Fig. 5a**), indicating a strong impact of *OsGELP87* on tiller and panicle development. By contrast, flag leaf length remained unchanged across all genotypes (**Fig. 5b**). Seed size was also affected in *osgelp87.3* compared to WT (**Fig. 5c, S17**). Panicle length was consistently shorter in *osgelp87.3* relative to WT (**Fig. 5d, 5e**), as well as the pollen number, further supporting the role of *OsGELP87* in reproductive development. However, the weight of 100 seeds was not significantly different between WT and genome-edited plants (**Fig. 5f**), suggesting that seed filling and grain density were not compromised. Together, these findings demonstrate that disruption of *OsGELP87* not affected the plants elongation, while exerting minimal effects on leaf architecture or seed weight, thereby pinpointing its specific contribution to reproductive productivity in rice.

Genome-edited *OsGELP87* alters lipid metabolism

Nile red staining was used to visualize lipid droplets (LD). LD are intracellular organelles that store neutral lipids, primarily triglycerides (TAG) and sterol esters (Klemm and Carvalho, 2024). Nile red staining demonstrated predominant accumulation of lipids in the fertile pollen within the locule (**Fig. S18**), pollen tube and pollen sac, but only weak scattered signals appeared in sterile pollen, stigma and filament (**Fig. 6a, and S18**). The intense lipid signal was observed on the surface of pollen grains, corresponding to the lipid-rich pollen coat, whereas stigma and filaments showed only weak, scattered signals, suggesting a limited lipid content (**Fig. S18**). In contrast, WT pollen showed uniform and abundant lipid accumulation, whereas ***osgelp87.3*** mutants displayed strongly reduced lipid signals (**Fig. S19a**) and a significant decrease in lipid-accumulated area (**Fig. S19b**) and normal intine formation (**Fig. S19c**) in *osgelp87*.3 was significantly lower percentages compared with WT, indicating impaired lipid organization during pollen maturation (**Fig. S19**c). The WT pollen accumulated abundant LDs, retained intact nuclei, and exhibited well-structured exine-intine layers (**Fig. 6a, S20**). However, the pollens of the *osgelp87.3* plants showed drastically reduced lipid accumulation, abnormal nuclear morphology, and disrupted

intine architecture relative to those of the WT (**Fig. 6a, S19, and S20**). According to Li et al. (2022), LDs are predominantly composed of TAGs, suggesting that *OsGELP87* contributes to TAG metabolism during gametophyte development.

Calcofluor White staining showed comparable pollen cell wall signals between WT and ***osgelp87.3*** mutants, indicating that cell wall formation is not disrupted (**Fig. 6a, S21**). However, ***osgelp87.3*** mutants exhibited abnormal pollen morphology and an increased proportion of sterile pollen, suggesting a defect in pollen maturation rather than cell wall biosynthesis (**Fig. S21**). Fluorescein diacetate (FDA) staining is used to detect the accumulation of esterase activity, as the non-fluorescent FDA is hydrolyzed by intracellular esterases into fluorescent fluorescein (Jones et al., 2016).

As shown in **Fig. 7a**, nuclear divisions from meiosis to mature pollen revealed that disruption of *OsGELP87* did not impair the early stages of microsporogenesis, since both WT and *osgelp87.3* plants (**Fig. 7a**) produced normal pollen mother cells (PMCs) and tetrads (**Fig. 7a**). However, in the *osgelp87.3* plants, microspores were often found to exhibit abnormal nuclear morphology due to remaining in an uninuclear stage (**Fig. 7a**). These abnormalities intensified during the young pollen and mature pollen stages, leading to a significant proportion of aborted pollen grains (**Fig. 7a**). The progressive collapse of pollen development in *osgelp87* plants was consistent with the proposed role of *OsGELP87* in lipid mobilization and pollen coat formation.

Loss of *OsGELP87* perturbs expression of genes critical for pollen and anther fertility

RNA-seq analyses were performed using anthers from both *osgelp87.3* and WT plants. The results of the transcriptome analysis showed a high correlation in gene expression between WT and *osgelp87*.3 (r = 0.914) (**Fig. S23a**). Screening relative to WT identified 23 rice genes with upregulated differential expression (up-DEGs) and 13 genes with downregulated differential expression (down-DEGs) in *osgelp87.3* compared with WT (**Fig. 8a; S23b**). The greater number of up-DEGs suggests that this gene is involved in feedback mechanisms as well as being upstream of lipid metabolism. The top eight up-DEGs were all anther-specific expression genes, while

three of the down-DEGs were also anther-specific expression genes (**Fig. 8a; S23b; Table S2**). Interestingly, multiple lipid transfer protein genes, including *OsLTP1.12*, *OsLTP1.13*, and *OsLTP1.20*, were up-regulated in the *osgelp87*.3 plant, whereas the four genes (*OSC6*, *OsLTP1.3*, *OsLTPd11*/*OsLTP6*, and *OsLTP1.4*) were down-regulated. Additionally, starch related genes expressed in the anther, such as *WX1*, *Os12BGlu38*, *OsSTA246*, *OsINV4*, and *OsIPP3*, *Os12BGlu38* and *OsSTA24* were detected as up-DEGs in the *osgelp87* plant. The mutation at the *OsGELP87* gene also affected the expression of the anthocyanin synthesis genes, *OsPAL1* and *OsDFR3*.

To validate the differences in transcriptional activities observed by RNA-seq analyses, qRT-PCR analysis was carried out with the four selected genes revealed marked differences between *osgelp87.3* and WT (**Fig. 9**). The *OsGELP87* expression of the genome-edited plant was upregulated, consistent with disruption of its normal regulation (**Fig. 9a**). Expression of *OsRboh1*, a gene encoding a respiratory burst oxidase implicated in ROS signalling, was also elevated in *osgelp87.3* (**Fig. 9b**). In contrast, both *OsAPX1* (ascorbate peroxidase 1), a key antioxidant enzyme, and *FAD2* (fatty acid desaturase 2), an enzyme central to unsaturated fatty acid biosynthesis, were markedly downregulated in the genome-edited plant (**Fig. 9c, d**). These transcriptional changes suggest that the genome editing of *OsGELP87* widely perturbs lipid metabolic processes and redox balance, thereby compromising pollen development and viability.

Co-expression analysis

RiceFREND database (https://ricefrend.dna.affrc.go.jp/) showed that *OsGELP87 (Os06g0636700)* is coexpressed with genes involved in lipid metabolism, carbohydrate processing, and stress responses (**Fig. S24**), suggesting a role in maintaining metabolic balance during reproductive development and abiotic stress. Notably, *OsLACS2*, an acyl-CoA synthetase, displays strong coexpression with *OsGELP87*, indicating coordinated functions in lipid turnover, where *OsGELP87* may release fatty acids that *OsLACS2* subsequently activates (**Fig. S24**). Co-expression with *OsCIN2*, a cell wall invertase, links *OsGELP87* to carbohydrate metabolism and energy supply, while association with the transcription factor *OsWR2* further supports involvement in wax and cutin biosynthesis. Together, these relationships suggest that *OsGELP87* acts at the

intersection of lipid and carbohydrate metabolism to support pollen development and enhance abiotic stress tolerance during the booting stage **(Fig. S23**).

DISCUSSION (1116 words)

Rationale for the non-redundancy of *OsGELP87*

We focused on *OsGELP87* because a previous transcriptome analysis of rice anthers (Yamamori et al., 2025) identified this gene as one of the most strongly expressed during the booting stage, a critical developmental window for pollen wall formation and male fertility. This expression pattern suggested that *OsGELP87* plays an important role during late pollen development. Consistent with this hypothesis, phylogenetic analysis of plant GDSL esterase/lipase (GELP) family members revealed that *OsGELP87* lacks a closely related paralog, indicating minimal functional redundancy in the rice genome. In addition, no natural loss-of-function (LOF) alleles of *OsGELP87* were detected among the 3,000 rice genomes surveyed, implying strong purifying selection acting on this locus. We have not obtained any complete knockout plants, either.

No plants were regenerated when exon 1 was targeted using CRISPR/Cas9, while mutated plants were produced when exon 2 and 3 were targeted. CRISPR/Cas9-generated *osgelp87.2* mutants targeted to exon 2 exhibited more severe phenotypes and produced few fertile seeds. However, the *osgelp87.3* mutants targeted to exon 3 avoided complete male sterility, instead exhibiting partial sterility and producing a fraction of viable pollen. Although pollen tube elongation was significantly reduced, fertilization was not entirely abolished. This phenotype suggests that the generated alleles retain residual activity or that limited compensatory mechanisms partially support pollen function. Nevertheless, reduced pollen tube growth is expected to impose a strong disadvantage during in vivo fertilization, where multiple pollen tubes compete within the style (Hayashi and Palmgren, 2021 and Dumais, 2021). Such reduced competitiveness provides a plausible explanation for why complete LOF alleles of *OsGELP87* are absent from natural populations, as pollen carrying such alleles would be consistently eliminated during reproductive competition.

OsGELP87 as a putative extracellular GDSL lipase

According to the characteristic amino acid motifs (WoLF PSORT, Plant-mPLoc, and DeepLoc), *OsGELP87* is predicted to encode a secreted GDSL esterase/lipase that is secreted and localized at the cell wall–locule interface. This is a region where cuticular lipids, sporopollenin precursors, and pollen wall components accumulate (Geitmann and Basic., 2023). This localization suggests that *OsGELP87* is likely to participate in the remodeling of secreted lipid substrates required for anther cuticle formation and pollen wall assembly. Similar extracellular GDSL enzymes have been reported in other plant systems, such as tomato CD1, which contributes to cutin biosynthesis at the fruit epidermis (Yeast et al., 2014). Together, these parallels support the idea that OsGELP87 represents a member of a specialized subgroup of GELPs adapted for apoplastic lipid processing.

Although direct enzymatic activity was not assessed in this study, the cytological and genetic evidence is consistent with a role for *OsGELP87* in modifying the extracellular lipid environment. Rather than acting as a sole regulatory factor, *OsGELP87* is more appropriately viewed as a central component within a broader lipid-processing system that supports pollen wall integrity.

Implication of co-expression with the cell-wall invertase gene

Co-expression analysis revealed that OsGELP87 is strongly associated with OsCIN2, a cell-wall invertase involved in sucrose cleavage and carbon partitioning (**Fig. S24**). While OsGELP87 is unlikely to directly catalyze sugar hydrolysis, this co-expression pattern suggests metabolic coordination between carbohydrate utilization and lipid remodeling. Pollen development during the vacuolated uninucleate to bicellular transition requires substantial energy and biosynthetic input, and coupling sugar metabolism to lipid processing could be essential for sustaining these demands (Ranjan et al., 2022). In addition, previous studies have demonstrated that some GELPs function as esterases acting on a broad range of substrates, including carbohydrate-derived esters (Tsugama et al. (2020); Rastogi et al., (2022)). Therefore, it remains possible that OsGELP87 contributes more generally to modifying ester linkages at the pollen wall

interface, indirectly influencing the physicochemical properties required for proper wall maturation.

Requirement of OsGELP87 at late stage in pollen development

Cytological analyses demonstrated that *OsGELP87* is dispensable for early microsporogenesis but becomes critical during late pollen development. Pollen mother cells, tetrads, and early microspores in *osgelp87* mutants were indistinguishable from those of the WT, whereas defects became evident at the vacuolated uninucleate stage (**Fig. 7**). These defects progressively intensified, leading to reduced lipid accumulation, abnormal nuclear morphology, impaired intine formation, and pollen collapse (**Fig. 6).** These observations indicate that *OsGELP87* is required for maintaining lipid homeostasis and structural integrity during late pollen maturation (**Fig. 10a**). Disrupted lipid accumulation was closely associated with nuclear abnormalities, consistent with previous reports showing that defects in lipid metabolism frequently precede late-stage pollen abortion (Wang et al., 2008). Reduced panicle number in *osgelp87* mutants reflect indirect consequences of impaired pollen fertility or altered reproductive resource allocation, rather than a direct role of *OsGELP87* in vegetative branching. Thus, *OsGELP87* appears to contribute to metabolic buffering processes that sustain pollen viability during the final stages of development.

Potential roles in pollen germination, tube growth, and lipid turnover

In addition to its role during pollen wall formation, *OsGELP87* may also contribute to pollen maturation and germination by supporting triacylglycerol (TAG) mobilization (**Fig. 10b**). TAG hydrolysis provides diacylglycerol, monoacylglycerol, and free fatty acids that serve as substrates for membrane biogenesis during pollen germination and tube extension (Bai et al., 2023). The reduced pollen tube elongation observed in *osgelp87* mutants is consistent with impaired lipid supply for these processes (**Fig. 10b**).

Furthermore, lipid turnover can generate signaling molecules such as phosphatidic acid, jasmonic acid, and lysophosphatidic acid, which are known regulators of pollen tube growth. Although direct evidence for altered signaling lipid levels is lacking, the

phenotypic data disruption of lipid-dependent signaling pathways. The strong transcriptional induction of the anther-specific lipid transfer protein gene OsC6 in *osgelp87* mutants suggests a potential compensatory response aimed at maintaining extracellular lipid flux, although a general stress response cannot be excluded (**Fig. 11**).

Linkage with lipid–redox networks and environmental adaptation

Gene expression analyses further place *OsGELP87* within a broader lipid–redox regulatory network. In *osgelp87* mutants, reduced expression of *FAD2* (**Fig. 9d**) and *OsAPX1* (**Fig. 9c**), together with strong induction of *OsRboh1* (**Fig. 9b**), indicates altered fatty-acid desaturation, weakened antioxidant capacity, and elevated reactive oxygen species (ROS) production. Excess ROS is known to compromise pollen development (Sankaranarayanan et al., 2020), suggesting that *OsGELP87* contributes indirectly to maintaining redox homeostasis during reproductive growth.

Other GELP family members involved in anther development, including *OsGELP34* (Zhang et al., 2020), *OsGELP110*/115 (Zhang et al., 2020), and Arabidopsis *AtGELP77* (Tsugama et al., 2020), similarly influence lipid metabolism and pollen fertility, supporting the notion that GELPs play conserved roles in reproductive lipid homeostasis. The strong evolutionary constraint observed for *OsGELP87*, together with its expression during the booting stage, suggests that this gene contributes to stabilizing pollen development under fluctuating environmental conditions, such as low temperature stress. Consequently, *OsGELP87* is promising target for understanding the genetic basis of reproductive robustness and climate resilience in rice.

CONCLUSION (78 words)

Our results indicate that *OsGELP87* is a non-redundant, evolutionarily conserved component of the lipid metabolic network required for late pollen development in rice. Rather than acting as a single master regulator, *OsGELP87* likely functions as an integral part of a coordinated system linking lipid remodeling, energy metabolism, redox balance, and pollen competitiveness. Disruption of this system compromises pollen maturation and fertilization efficiency, providing a mechanistic explanation for the strong purifying selection acting on *OsGELP87* in natural rice populations.

MATERIAL AND METHOD (1127 words)

Bioinformatic analysis of target genes

Target gene sequences were analyzed using BLAST (NCBI; https://blast.ncbi.nlm.nih.gov/) to confirm sequence identity and retrieve homologs, and gene expression profiles were obtained from RiceXPro (https://ricexpro.dna.affrc.go.jp/). Multiple sequence alignment of GDSL lipase/esterase amino acid sequences from rice and other plant species was performed using ClustalW in MEGA v.11. An unrooted phylogenetic tree was constructed using the Neighbor-Joining method with Poisson-corrected evolutionary distances, pairwise deletion for gaps and missing data, and 1000 bootstrap replicates to assess statistical support. Signal peptides of the genes were predicted using SignalP (http://www.cbs.dtu.dk/services/SignalP/) and protein domain architecture was analyzed using Pfam (https://pfam.xfam.org/) and SMART (https://smart.embl.de/help/smart_about.shtml) databases.

Haplotype Analysis

All data, including average latitude, haplotypes, subpopulation SNPs, and country of origin, were obtained from the IRRI SNP-seek Database (3K rice genome dataset) (https://snpseek.irri.org). Haplotypes of the *OsGELP87* gene were defined based on SNPs from this database. Rice varieties such as A58; Supa; Nene; Kasalat; I33; Kirara; PL9; Koshihikari; T65; Kitaake; Kitakaori; Lambyque and Silewah were mapped to the Nipponbare reference genome using Bowtie 2, and SNPs were called with GATK4 HaplotypeCaller. SNPs were further analyzed using TASSEL 5 and IGV to identified the haplotype group based on SNPseek database. Haplotype sequences were aligned using ClustalW in MEGA 11, and haplotype networks were constructed with PopArt to assess genealogical relationships. Haplotype diversity was calculated with DnaSP v6. Rice accessions were classified into 12 subpopulations: aro, aus, admix, ind1A, ind1B, ind2, ind3, indica-X (indx), japx, subtrop, temp, and trop. These subpopulations reflect geographic and agronomic distinctions, e.g., aro (fragrant, South Asia), aus (early-maturing, drought-tolerant, Bangladesh/India), admix (hybrids worldwide), indica

562 subgroups (mainly South and Southeast Asia), japx (japonica admixed, East Asia),
563 subtrop (mild climates), temp (temperate, cold-tolerant), and trop (tropical, long-grain,
564 hot/humid regions). Some varieties representing each haplotype were grown in isolation
565 greenhouse in Hokkaido (Latitude 43°) (about 25°C day / 22°C night) to assess pollen
566 fertility and agronomic traits.
567
568 **CRISPR/Cas9-mediated rice transformation**
569 The sgRNA targeting *OsGELP87* were designed using CHOPCHOP
570 (https://chopchop.cbu.uib.no/) and cloned into pMR185-pENTR_L1L2_OsChimera 2
571 with 5′ overhangs, then recombined into pMR426_pHZmUCAS9PLUS-OLE-Citrine
572 using Gateway LR Clonase II. Constructs were transformed into DH5α E. coli for
573 verification by Sanger sequencing. Mature seeds of *Oryza sativa* L. cv. Nipponbare
574 were dehulled, surface-sterilized, and cultured on N6D medium to induce callus
575 formation. Plasmids were introduced into *Rhizobium radiobacter* LBA4404, and calli
576 were infected with Agrobacterium and co-cultivated on N6As medium, followed by
577 selection on hygromycin-containing N6S medium and regeneration on differentiation
578 medium. All the primers and the sgRNA sequences were listed on **Table S1**.
579 Transgenic plants were screened by PCR for hygromycin and Cas9, and target loci were
580 amplified using KOD Fx Neo DNA Polymerase for Sanger sequencing. Mutations were
581 analyzed with SnapGene and quantified using the ICE tool (Synthego,
582 https://ice.editco.bio/#/).
583
584 **RNA-seq and qRT-PCR analysis**
585 Anthers from WT and *osgelp87*.3 plants were collected at the same developmental stage
586 from the third to fifth spikelet of primary rachis branches, immediately frozen in liquid
587 nitrogen, and stored at −80 °C. For RNA sequencing, samples were collected in
588 triplicate, with each replicate consisting of pooled anthers from multiple plants. For
589 quantitative RT–PCR analysis, total RNA was isolated from shoots, leaves, roots, and
590 anthers, and gene expression was analyzed using a real-time PCR system with gene-
591 specific primers for *OsGELP87*, *FAD2*, *OsAPX1*, and *OsRboh1*.
592
593 **Protein structure prediction**

The amino acid sequences of the WT and genome-edited plant proteins were used to predict their three-dimensional (3D) structures. Structural models were generated using **AlphaFold** (https://alphafold.ebi.ac.uk), and the resulting 3D structures were visualized and compared using **ChimeraX** (https://www.cgl.ucsf.edu/chimerax/) to assess conformational differences. This approach allowed the identification of structural changes caused by mutations and facilitated interpretation of their potential functional impact.

Microscopy

Anthers were collected at the target developmental stages and immediately fixed in MTSB (50 mM PIPES, 5 mM EGTA, 5 mM $MgSO_4$, pH 6.9) or FAA, followed by seven rounds of 2 min vacuum infiltration, washed three times with PBS (137 mM NaCl, 2.7 mM KCl, 10 mM Na_2HPO_4, 1.8 mM KH_2PO_4, pH 7.4) under vacuum for 5 min each, and stored at 4 °C until further processing. Lipids were visualized by crushing anthers and staining with 1–5 µg/mL Nile Red in PBS or 50% glycerol for 10–30 min in the dark, followed by brief PBS rinses and fluorescence microscopy. Esterase's activity was assessed using 5–10 µg/mL fluorescein diacetate (FDA) for 5–10 min in the dark, and viable cells were observed by green fluorescence. The pollen intine was stained with 0.1% Calcofluor White and 10% KOH for 15 min at room temperature, and images were analyzed with ImageJ to calculate the intine-to-pollen area ratio; pollen with <20–30% fluorescence or irregular patterns was classified as intine-defective. Nuclei were visualized in FAA-fixed anthers permeabilized with 0.1% Triton X-100 and stained with 1 µg/mL DAPI for 10–20 min in the dark, using a KEYENCE fluorescence microscope. Reactive oxygen species (ROS) accumulation was detected using 1 mg/mL DAB (pH 3.8) with 5 min vacuum infiltration and 4–6 h incubation in the dark, followed by ethanol clearing and light microscopy to visualize brown precipitates. To assess anther and pollen morphology, anther length and pollen diameter were measured in WT and genome-edited plants; pollen grains were classified as fertile or sterile, imaged under a calibrated light microscope, and quantitatively analyzed using ImageJ.

Pollen grains were stained with 1.5% KI and 0.15% I_2 (Lugol's solution) and observed under an Olympus BX53 microscope. Dark, round grains were scored as fertile, while unstained, lightly stained, or irregular grains were considered sterile; fertility was calculated as the percentage of fertile grains from at least nine flowers per line. Spikelet fertility was determined by counting filled spikelet in three panicles per plant (two random, one from the main culm) after drying at 50 °C for 7 days. For pollen viability and germination, pollen was collected immediately after floret opening and cultured for 30 min at 30 °C in a medium containing 20% sucrose, 10% PEG 4000, 3 mM $Ca(NO_3)_2$, 40 mg L^{-1} H_3BO_3, and 3 mg L^{-1} vitamin B_1 (pH 5.8). Samples were observed under an Olympus BX50 microscope, and images with ≥15 grains were used to calculate germination rates and assess pollen integrity.

Characterization of the phenotypes

Morphological traits, including plant height (cm), heading date (days after planting, DAP), number of panicles (n), panicle length (cm), and seed length (cm), were measured for WT and genome-edited plants. For seed germination assays, sterilized seeds were placed on moistened filter paper in Petri dishes and incubated at 28°C under controlled humidity. Germination percentage was recorded daily from 0 to 7 days after sowing (DAS) and calculated as the number of germinated seeds divided by the total number of seeds.

Statistical analysis

To assess the statistical significance of the associations between genotypes (WT and genome-edited plants), one-way analysis of variance (ANOVA), paired and unpaired t-tests, and Duncan's Multiple Range Test (DMRT) were performed. Data analyses were conducted using Microsoft Excel and R Studio.

REFERENCES

Ariizumi T, Toriyama K. (2011) Genetic regulation of sporopollenin synthesis and pollen exine development. Annual Review of Plant Biology, 62:437–460. https://doi.org/10.1146/annurev-arplant-042809-112312

Bai M, Gao H, Yang Y, Wu H. (2023) Changes in the content of pollen total lipid and TAG in Arabidopsis thaliana dgat1 mutant. AoB PLANTS, 15:plad012. https://doi.org/10.1093/aobpla/plad012

Chepyshko H, Lai C-P, Huang L-M, Liu J-H, Shaw JF (2012) Multifunctionality and diversity of GDSL esterase/lipase gene family in rice (Oryza sativa L. japonica) genome: New insights from bioinformatics analysis. BMC Genomics, 13:309. https://doi.org/10.1186/1471-2164-13-309

Duan L, Wang F, Shen H, Xie S, Chen X, Xie Q, Li R, Cao A, Hongbin L (2023) Identification, evolution, and expression of GDSL-type esterase/lipase (GELP) gene family in three cotton species: A bioinformatic analysis. BMC Genomics, 24:795. https://doi.org/10.1186/s12864-023-09717-3

Dumais J (2021) Mechanics and hydraulics of pollen tube growth. New Phytologist, 232:1549-1565. https://doi.org/10.1111/nph.17722

Gao M, Yin X, Yang W, Lam SM, Tong X, Liu J, Wang X, Li Q, Shui G, He Z (2017) GDSL lipases modulate immunity through lipid homeostasis in rice. PLoS Pathogens, 13: e1006724. https://doi.org/10.1371/journal.ppat.1006724

Geitmann A, Bacic A (2023) Focus on cell walls. Plant Physiology, 194:1–4. https://doi.org/10.1093/plphys/kiad537

Hayashi M, Palmgren, M. (2021) The quest for the central players governing pollen tube growth and guidance. Plant Physiology, 185:682–693. https://doi.org/10.1093/plphys/kiaa09

He ZD, Tao ML, Leung DWM, Yan XY, Chen L, Peng XX, Liu EE (2021) The rice germin-like protein OsGLP1 participates in acclimation to UV-B radiation. Plant Physiology, 186:1254–1268. https://doi.org/10.1093/plphys/kiab125

Huo Y, Pei Y, Tian Y, Zhang Z, Li K, Liu J, Xiao S, Chen H, Liu J (2020) IRREGULAR POLLEN EXINE2 encodes a GDSL lipase essential for male fertility in maize. Plant Physiology, 184:1438–1454. https://doi.org/10.1104/pp.20.00105

Jones KH, Senft JA (1985) An improved method to determine cell viability by simultaneous staining with fluorescein diacetate–propidium iodide. The Journal of Histochemistry and Cytochemistry, 33:77–79.

Lee SK, Shim SH, Eom JS, Cho JI, Kwak JU, Eom SC, Jeon JS (2024) Cell wall invertases from maternal tissues modulate sucrose flux in apoplastic pathways during rice anther and seed development. International Journal of Molecular Sciences, 25:11557. https://doi.org/10.3390/ijms252111557

Li YF, et al. (2024). Flowering time regulator qFT13-3 involved in soybean adaptation to high latitudes. Plant Biotechnology Journal, 22:1164–1176. https://doi.org/10.1111/pbi.14254

Ling S, Chen C, Wang Y, Sun X, Lu Z, Ouyang Y, Yao J (2015) The mature anther-preferentially expressed genes are associated with pollen fertility, pollen germination, and anther dehiscence in rice. BMC Genomics, 16:1–15. https://doi.org/10.1186/s12864-015-1305-y

Lubba KM, Yamamori K, Kishima Y (2025) Haplotype shifts in the lipid-related OsGELP gene family underpin rice adaptation to high latitudes. Scientific Reports, 15:32293. https://doi.org/10.1038/s41598-025-15488-6

Missaoui K, Gonzalez-Klein Z, Pazos-Castro D, Hernandez-Ramirez G, Garrido-Arandia M, Brini F, Diaz-Perales A, Tome-Amat J (2022) Plant non-specific lipid transfer proteins: An overview. Plant Physiology and Biochemistry, 171:115–127. https://doi.org/10.1016/j.plaphy.2021.12.026

Park JJ et al. (2010) Mutation in Wilted Dwarf and Lethal 1 (WDL1) causes abnormal cuticle formation and rapid water loss in rice. Plant Molecular Biology, 74:91–103. https://doi.org/10.1007/s11103-010-9656-x

Quilichini TD, Grienenberger E, Douglas CJ (2015) The biosynthesis, composition, and assembly of the outer pollen wall: A tough case to crack. Phytochemistry, 113:170–182. https://doi.org/10.1016/j.phytochem.2014.05.002

Ranjan R, Malik N, Sharma S, Agarwal P, Kapoor S, Tyagi AK (2022) OsCPK29 interacts with MADS68 to regulate pollen development in rice. Plant Science, 321:111297. https://doi.org/10.1016/j.plantsci.2022.111297

Rastogi L, Chaudhari AA, Sharma R et al. (2022) Arabidopsis GELP7 functions as a plasma membrane–localized acetyl xylan esterase, and its overexpression improves saccharification efficiency. Plant Molecular Biology, 109:781–797. https://doi.org/10.1007/s11103-022-01275-8

Sankaranarayanan S, Ju Y, Kessler SA (2020) Reactive oxygen species as mediators of gametophyte development and double fertilization in flowering plants. Frontiers in Plant Science, 11:1199. https://doi.org/10.3389/fpls.2020.01199

Shen G, Sun W, Chen Z, Shi L, Hong J, Shi J (2022) Plant GDSL esterases/lipases: Evolutionary, physiological, and molecular functions in plant development. Plants, 11:468. https://doi.org/10.3390/plants11040468

Shi J, Cui M, Yang L, Kim YJ, Zhang D (2015). Genetic and biochemical mechanisms of pollen wall development. Trends in Plant Science, 20:741–753. https://doi.org/10.1016/j.tplants.2015.07.010

Shim SH, Mahong B, Lee SK, Kongdin M, Lee C, Kim YJ, Qu G, Zhang D, Ketudat Cairns JR, Jeon JS (2022). Rice β-glucosidase Os12BGlu38 is required for synthesis of intine cell wall and pollen fertility. Journal of Experimental Botany, 73:784–800. https://doi.org/10.1093/jxb/erab439

Tsugama D, Fujino K, Liu S, Takano T. (2020) A GDSL-type esterase/lipase gene, GELP77, is necessary for pollen dissociation and fertility in Arabidopsis. Biochemical and Biophysical Research Communications, 526:1036–1041. https://doi.org/10.1016/j.bbrc.2020.03.179

Wang R, Dobritsa AA (2021) Loss of THIN EXINE2 disrupts multiple processes in the mechanism of pollen exine formation. Plant Physiology, 187:133–157. https://doi.org/10.1093/plphys/kiab244

Wang Y, Wu H, Yang M (2008) Microscopy and bioinformatic analyses of lipid metabolism implicate a sporophytic signaling network supporting pollen development in Arabidopsis. The Plant Cell, 20:667–674. https://doi.org/10.1105/tpc.107.056028

Xu J, Ding Z, Vizcay-Barrena G, Shi J, Liang W, Yuan Z, Werck-Reichhart D, Schreiber L, Wilson Z A, Zhang D (2014) ABORTED MICROSPORES acts as a master regulator of pollen wall formation in Arabidopsis. The Plant Cell, 26:1544–1556. https://doi.org/10.1105/tpc.114.122986

Xu J, Yang C, Yuan Z, Zhang D, Gondwe MY, Ding Z, Liang W, Zhang D, Wilson ZA (2010) The ABORTED MICROSPORES regulatory network is required for postmeiotic male reproductive development in Arabidopsis thaliana. The Plant Cell, 22:91–107. https://doi.org/10.1105/tpc.109.071803

Yamamori K, Ishiguro S, Ogasawara K, Lubba KM, Fujino K, Onishi K, Sato Y, Kishima Y (2025). Anther transcriptomes in cold-tolerant rice cultivars tend to show insensitive responses. Plant Stress, 15:100700. https://doi.org/10.1016/j.stress.2024.100700

Yeats TH, Huang W, Chatterjee S, Viart HM-F, Clausen MH, Stark RE, Rose JKC (2014) Tomato Cutin Deficient 1 (CD1) and putative orthologs comprise an ancient family of cutin synthase-like (CUS) proteins that are conserved among land plants. The Plant Journal, 77:667–675. https://doi.org/10.1111/tpj.12422

Yuan G et al. (2020) A rice GDSL esterase/lipase protein (GELP) is required for anther and pollen development. Molecular Breeding, 40:90. https://doi.org/10.1007/s11032-020-01170-4

Zhang H, Wang M, Li Y, Yan W, Chang Z, Ni H, Chen Z, Wu J, Xu C, Deng XW, Tang X (2020) GDSL esterase/lipases OsGELP34 and

OsGELP110/OsGELP115 are essential for rice pollen development. Journal of Integrative Plant Biology, 62:1574–1593. https://doi.org/10.1111/jipb.12919

Zhang L, Liu Y, Wei G, Lei T, Wu J, Zheng L, Ma H, He G, Wang N (2022) POLLEN WALL ABORTION 1 is essential for pollen wall development in rice. Plant Physiology, 190:2229–2245. https://doi.org/10.1093/plphys/kiac435

Zhou Y, Dobritsa AA (2025) Forging the pollen fortress: Cell biological mechanisms of exine formation. Current Opinion in Plant Biology, 86:102742. https://doi.org/10.1016/j.pbi.2025.102742

STATEMENTS & DECLARATIONS

FUNDING

This work was supported by JSPS KAKENHI grants (19H00937 and 23H02180) and partially by SATREPS Rice BACS Project to Y.K.

COMPETING INTERESTS

The authors declare that they have no competing interests.

AUTHOR CONTRIBUTION

Kayyis Muayadah Lubba and Yuji Kishima made the concept of the study, designed the experimental plan. K.L.M. performed the experiments. The first draft of the manuscript was written by Kayyis Muayadah Lubba, and Yuji Kishima commented and amended on previous version. Kayyis Muayadah Lubba was supervised by Yuji Kishima.

DATA AVAILABILITY

All relevant data can be found within this article and supporting materials.

FIGURE LEGENDS (1413 words)

Fig. 1 Amino acid domain architecture and phylogenetic relationships of OsGELP87

(a) Characteristics of the OsGELP87 amino acid sequence and protein domain analysis, including the position of the signal peptide (SP). Protein domain architecture was analyzed using Pfam and SMART databases. **(b)** Phylogenetic tree of protein sequences most closely related to OsGELP87 across multiple species. Bootstrap probabilities were estimated by the neighbor-joining method with 1000 replications and constructed using MEGA X.

Fig. 2 Haplotype analysis of *OsGELP87*

(a) Haplotype variation of *OsGELP87* in rice 3K genomes. Schematic representation of the *OsGELP87* gene structure (top) showing exons (black boxes), untranslated regions (gray boxes), and the positions of SNPs (red vertical lines) across the non-coding and coding regions. Below, haplotypes are classified based on SNP patterns obtained from the 3K rice genome project. **(b)** Frequency of subpopulations in haplotypes, with the latitude averages evaluated by Tukey's range test. The subpopulation classification was based on Rice SNP-Seek database (https://snp-seek.irri.org/). Y axis indicates proportion of each subpopulation in the haplotype. **(c)** Haplotype network. The relative number of varieties included in each haplotype is indicated by the area of each circle. The length of the line connecting two circles represents the number of SNPs between two haplotypes. **(d)** Haplotypes distribution in worldwide accession based on Rice SNP seek data.

Fig. 3 Genome Editing Targets and Predicted Structural Impact in OsGELP87

(a) Genome editing position or sgRNA position (1.) *osgelp87.1*; (2.) *osgelp87.2a*; (3.) *osgelp87.2b*; and (4.) *osgelp87.3* **(b)** Alignment of WT and *osgelp87.3* edited sequences. Amino acid sequence alignment between the WT OsGELP87 and the *osgelp87* edited allele (*osgelp87.3*) is displayed. Asterisks (*) indicate conserved residues. Predicted S-palmitoylation sites are highlighted in yellow boxes. In the edited sequence, a premature stop codon is indicated, leading to a truncated C-terminal region shown in red. This truncation results in the loss or alteration of potential palmitoylation

motifs, which may affect the protein's lipid modification and membrane association properties. (**c**) Protein structure difference between WT and mutant *osgelp.3 (in 1bp A).* The red and yellow color showed the alpha helixes and blue color showed the beta sheet. The green color showed the two of alpha sheet that disappeared in mutant, orange color showed the signal peptide sequence. Structural models were generated using AlphaFold (https://alphafold.ebi.ac.uk), and the resulting 3D structures were visualized and compared using ChimeraX (https://www.cgl.ucsf.edu/chimerax/) to assess conformational differences.

Fig. 4 Phenotypic and cytological analysis of the *osgelp87* mutant compared to WT rice reproductive organs

(a) Morphological comparison of anthers (left), flower, pistil, and ovary (right) between WT and *osgelp87.3*. The mutant shows reduced anther size and abnormal floret morphology. **(b)** Microscopic observation of fertile and sterile pollen grains from WT and *osgelp87.3*. Fertile pollen exhibits a normal round shape, whereas sterile pollen appears shrunken and collapsed. Scale bar = 50 μm. **(c)** I_2–KI staining of pollen grains from WT and *osgelp87.3*, showing reduced pollen fertility and viability in the mutant. Scale bar = 20 μm. **(d)** Quantification of pollen fertility (%). **(e)** Pollen viability (%), **(f)** Pollen tube length (μm), **(g)** Pollen diameter (μm), and **(h)** Anther length (mm) in WT and *osgelp87.3*. **(i)** Seed fertility (%). Data represent mean ± SE (n ≥ 3 biological replicates). Statistical significance was determined using Student's *t*-test ($p < 0.05$; $p < 0.01$; ns, not significant).

Fig. 5 Loss of OsGELP87 causes severe defects in floral development and male fertility

(a) Number of panicles different **(b)** Flag leaf length of WT and *osgelp87* mutants. (**c**) Seed length of WT and *osgelp87.2* mutants. **(d)** Panicle length comparison between *osgelp87.3* mutant and WT. Different letters indicate significant differences ($P < 0.05$). (**e**) Pollen number per anther in WT and *osgelp87* mutants. (**f**) Weight of 100 seeds in WT and *osgelp87* mutants. Data are shown as mean ± SD. Asterisks indicate statistically significant differences compared with WT ($P < 0.05$; $^*P < 0.01$), while ns indicates no significant difference.

Fig. 6 Cytological characterization of pollen grains in the *osgelp87* mutant compared to WT rice

(a) Staining analysis of pollen grains using Sudan Black B (lipid bodies), Nile Red (lipid droplets, Ld), DAPI (nuclei: sperm nucleus [Sn], vegetative nucleus [Vn]), Calcofluor (cell wall components: exine [Ex], intine [In]), and FDA (viability). WT pollen exhibits normal lipid accumulation, nuclear integrity, and cell wall structure, whereas *osgelp87.3* pollen shows reduced lipid staining, abnormal nuclei, and weaker viability signals. Scale bar = 100 μm. **(b)** Quantification of lipid accumulation (μm³) in WT and *osgelp87.3* pollen grains. **(c)** Percentage of pollen grains with normal intine structure in WT and *osgelp87.3*. Data represent mean ± SE (n ≥ 3 biological replicates). Statistical significance was determined using Student's *t*-test (**$p < 0.001$).

Fig. 7 Abnormal pollen development in *osgelp87.3* mutants

(a) DAPI staining of male gametophytes at successive developmental stages, including pre-meiosis, tetrad, early and vacuolated uninucleate, early binucleate, and mature starch-filled pollen. Nipponbare (WT) exhibited normal nuclear division and progression, whereas *osgelp87.3* mutants displayed severe developmental defects, particularly from the vacuolated uninucleate to pollen maturity stages. **(b)** Quantification of normal versus abnormal pollen cells at each stage in WT and *osgelp87.3*. While early stages (Pollen Mother Cell (PMC), tetrad, MSP (Microspore) were largely unaffected, a marked increase in abnormal nuclei was observed in *osgelp87.3* during the young pollen (YP) and mature pollen (PM) stages (red arrowheads), coinciding with defective nuclear organization and aborted pollen grains. Data represent counts from multiple biological replicates.

Fig. 8 Transcriptome analysis of WT and *osgelp87.3* mutant rice

(a) Genes that are highly expressed in the WT but UPREGULATED in the osgelp87 mutant and Genes that are highly expressed in the WT but DOWNREGULATED in the osgelp87 mutant. **(b)** *Gene Ontology (GO) enrichment analysis of differentially expressed genes using ShinyGO.* The bar plot shows the top enriched biological processes ranked by fold enrichment. The x-axis represents fold enrichment, while the

color scale indicates the statistical significance (-log10 FDR). The most significantly enriched GO terms include pollen exine formation, pollen wall assembly, photosynthesis-related processes, and lipid transport, suggesting strong involvement of the gene set in pollen development and metabolic regulation.

Fig. 9 Quantitative RT-PCR analysis of selected genes in WT and *osgelp87* mutant rice

Relative expression levels of **(a)** *OsGELP87*, **(b)** *OsRboh1*, **(c)** *OsAPX1*, and **(d)** *FAD2* in WT and *osgelp87* plants. Gene expression was normalized to an internal control, and fold-change values are shown relative to WT. Data represent mean ± standard error (SE) of three biological replicates

Fig. 10 Proposed role of OsGELP87 in pollen coat formation, lipid metabolism, and pollen fertility

(a) Pollen Coat Formation and De-esterification of the Pollen Wall: OsGELP87 functions as a lipase and esterase enzyme, hydrolyzing lipophilic compounds during the tricellular stage of pollen development. These compounds contribute to sporopollenin and tryphine (pollen coat) formation, which are crucial for exine structure. Genome edited of OsGELP87 results in impaired pollen coat formation, leading to low pollen fertility and lipid accumulation. **(b)** Energy Mobilization in Pollen Germination: OsGELP87 hydrolyzes triacylglycerols (TAGs) in lipid droplets (LD) to generate diacylglycerol (DAG), monoacylglycerol (MAG), and free fatty acids, which provide energy and membrane components during pollen tube growth. Lipid-derived signaling molecules such as phosphatidic acid (PA), jasmonic acid (JA), lysophosphatidic acid (LPA), and others promote pollen tube development. KO of OsGELP87 disrupts these processes, resulting in low pollen germination and developmental defects.

Fig. 11 OsGELP87 regulates pollen wall formation and pollen germination in rice

Schematic representation of pollen development from mitosis I to pollen germination in WT rice, highlighting stage-specific gene networks involved in tapetal function, pollen wall formation, and pollen tube emergence. Black gene names indicate previously characterized genes known to function at each developmental stage. Genes shown in red

are significantly upregulated, whereas genes in blue are significantly downregulated in the *osgelp87* mutant compared with WT. During early anther development, key regulators of tapetum differentiation and sporopollenin biosynthesis (e.g., *AMS, GAMYB, MS1, ACOS5,* and *CYP703A* family genes) are active. At the binucleate and starch-filled pollen stages, genes associated with intine and exine formation, carbohydrate metabolism, and pollen wall assembly (including *CESA, PME/PMEI, RGP,* and *Os12BGlu38*) are engaged, with altered expression of *OsGELP87*–related pathways in the mutant. During pollen germination, genes involved in cell wall loosening and pollen tube elongation, such as *OSIPP3* and *OsExPB9*, show significant upregulation, while several lipid-transfer protein genes (*OsLTP1.12, OsLTP1.13,* and *OsLTP1.20*) are differentially regulated, indicating disrupted lipid and cell wall dynamics in *osgelp87*. Collectively, this model illustrates that OsGELP87 participates in coordinating pollen wall biogenesis and late-stage pollen germination processes by modulating multiple gene networks across developmental stages.

SHORT LEGENDS OF SUPPORTING FIGURES

Fig. S1 OsGELPs gene expression level

Fig. S2 Tissue-specific expression of *OsGELP87* determined by qRT-PCR

Fig. S3 In silico prediction of lipid modification sites and subcellular localization of OsGELP87

Fig. S4 Sequence alignment and expression profiles of rice GDSL lipase genes *OsGELP32* and *OsGELP87*

Fig. S5 Haplotype variation of *OsGELP87*

Fig. S6 Multiple sequence alignment of *OsGELP87* haplotypes showing conserved motifs and functional domains

Fig. S7 Predicted three-dimensional structures of *OsGELP87* haplotypes showing amino acid variations at key functional residues

Fig. S8 Sequence alignment of OsGELP87 WT and mutant proteins

Fig. S9 Generation and phenotypic analysis of *osgelp87* mutants

Fig. S10 Mutant *osgelp87.2a*

Figure S11. Mutant *osgelp87.2b*.

Fig. S12 Reduced pollen fertility and seed set in *osgelp87* mutants

Fig. S13 Pollen fertility and germination analysis in *osgelp87.3* mutant lines

Fig. S14 In vitro pollen germination assay showing pollen tube growth in WT and *osgelp87-3* mutants

Fig. S15 Stigma and pistil morphology in WT and *osgelp87.3* mutant rice

Fig. S16 Agronomic traits and seed germination analysis of the *osgelp87* mutant compared to WT rice

Fig. S17 The mature seed (after oven-dried) difference between WT and the mutants (scale bar: 1 cm)

Fig. S18 Nile Red staining reveals lipid distribution in the reproductive tissues of rice (cv. Nipponbare)

Fig. S19 OsGELP87 genome edited disrupts lipid distribution and intine formation in rice pollen

985 **Fig. S20 Nile red staining of WT and *osgelp87.3* mature pollen**

986

987 **Fig. S21 Calcofluor White Staining for WT and *osgelp87.3* mutant**

988

989 **Fig. S22 FDA staining of WT and *osgelp87.3* mature pollen**

990

991 **Fig. S23 Transcriptome analysis of WT and *osgelp87* mutant rice.**

992

993 **Fig. S24 Co-expression network and KEGG pathway annotation of Os11g0558300**
994 **(OsLACS2) in rice**

995

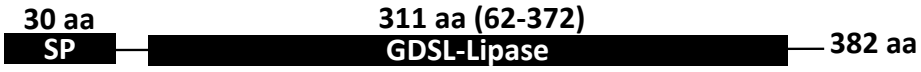
996 **Table S1 List primers and sequences**

997

998 **Table S2 RNA-seq expression of some flowering genes**

Main Figure

a.


30 aa
311 aa (62-372)
SP
GDSL-Lipase
382 aa

b.

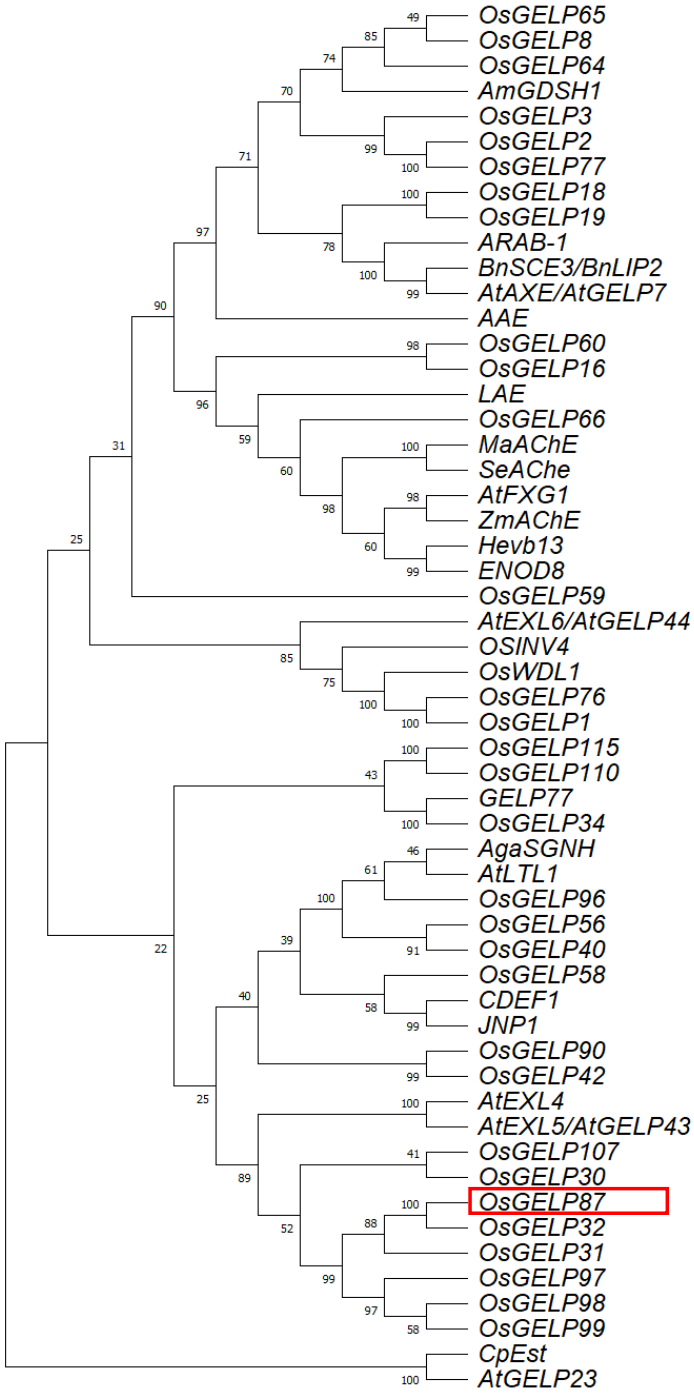

OsGELP65
OsGELP8
OsGELP64
AmGDSH1
OsGELP3
OsGELP2
OsGELP77
OsGELP18
OsGELP19
ARAB-1
BnSCE3/BnLIP2
AtAXE/AtGELP7
AAE
OsGELP60
OsGELP16
LAE
OsGELP66
MaAChE
SeAChe
AtFXG1
ZmAChE
Hevb13
ENOD8
OsGELP59
AtEXL6/AtGELP44
OsINV4
OsWDL1
OsGELP76
OsGELP1
OsGELP115
OsGELP110
GELP77
OsGELP34
AgaSGNH
AtLTL1
OsGELP96
OsGELP56
OsGELP40
OsGELP58
CDEF1
JNP1
OsGELP90
OsGELP42
AtEXL4
AtEXL5/AtGELP43
OsGELP107
OsGELP30
OsGELP87
OsGELP32
OsGELP31
OsGELP97
OsGELP98
OsGELP99
CpEst
AtGELP23

Fig. 1

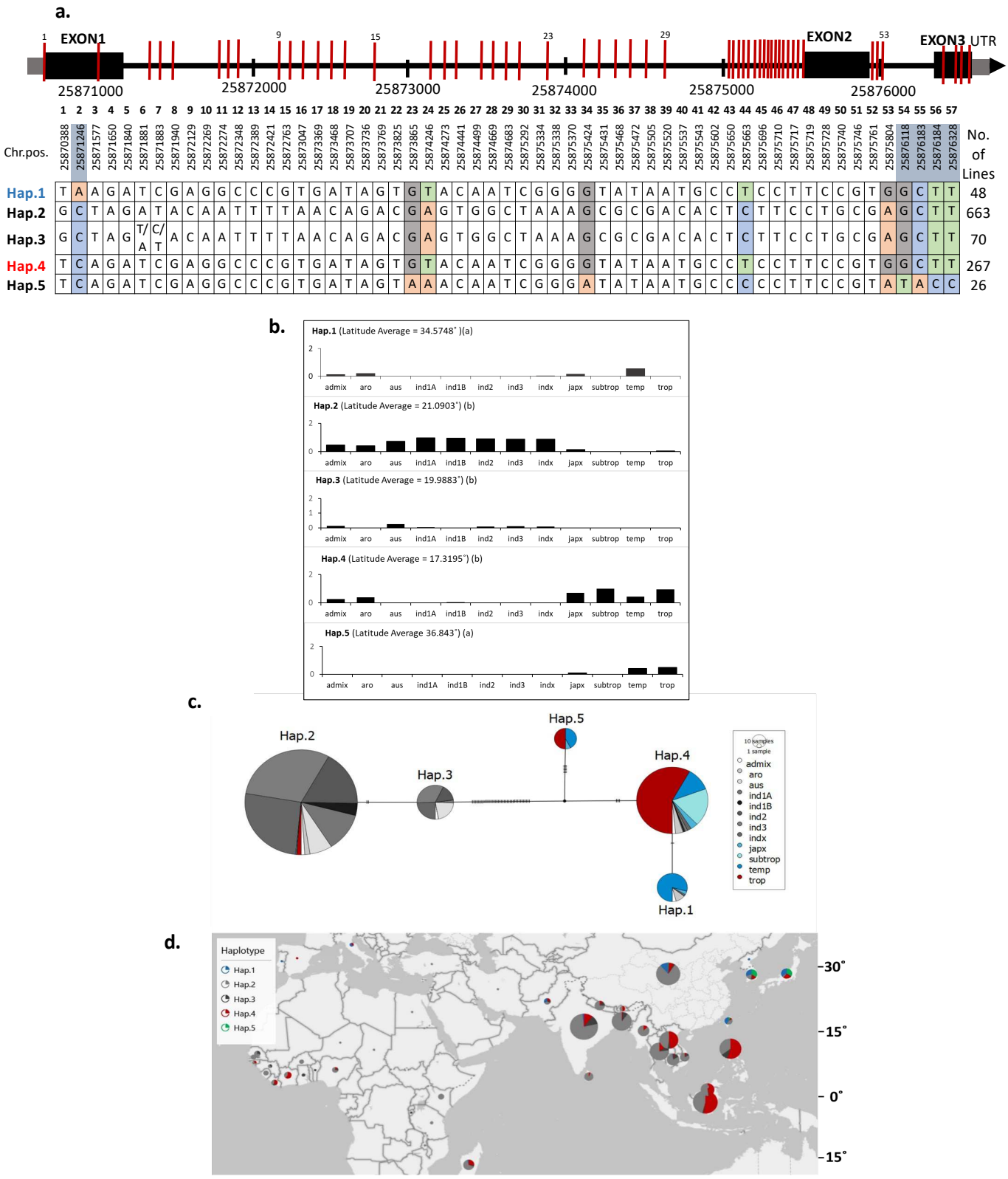

a.
EXON1
EXON2
EXON3 UTR
25871000
25872000
25873000
25874000
25875000
25876000
Chr.pos.
No. of Lines
Hap.1 48
Hap.2 663
Hap.3 70
Hap.4 267
Hap.5 26
b.
Hap.1 (Latitude Average = 34.5748˚)(a)
Hap.2 (Latitude Average = 21.0903˚) (b)
Hap.3 (Latitude Average = 19.9883˚) (b)
Hap.4 (Latitude Average = 17.3195˚) (b)
Hap.5 (Latitude Average 36.843˚) (a)
admix aro aus ind1A ind1B ind2 ind3 indx japx subtrop temp trop
c.
Hap.2
Hap.3
Hap.5
Hap.4
Hap.1
admix
aro
aus
ind1A
ind1B
ind2
ind3
indx
japx
subtrop
temp
trop
d.
Haplotype
Hap.1
Hap.2
Hap.3
Hap.4
Hap.5
30˚
15˚
0˚
-15˚

Fig. 2

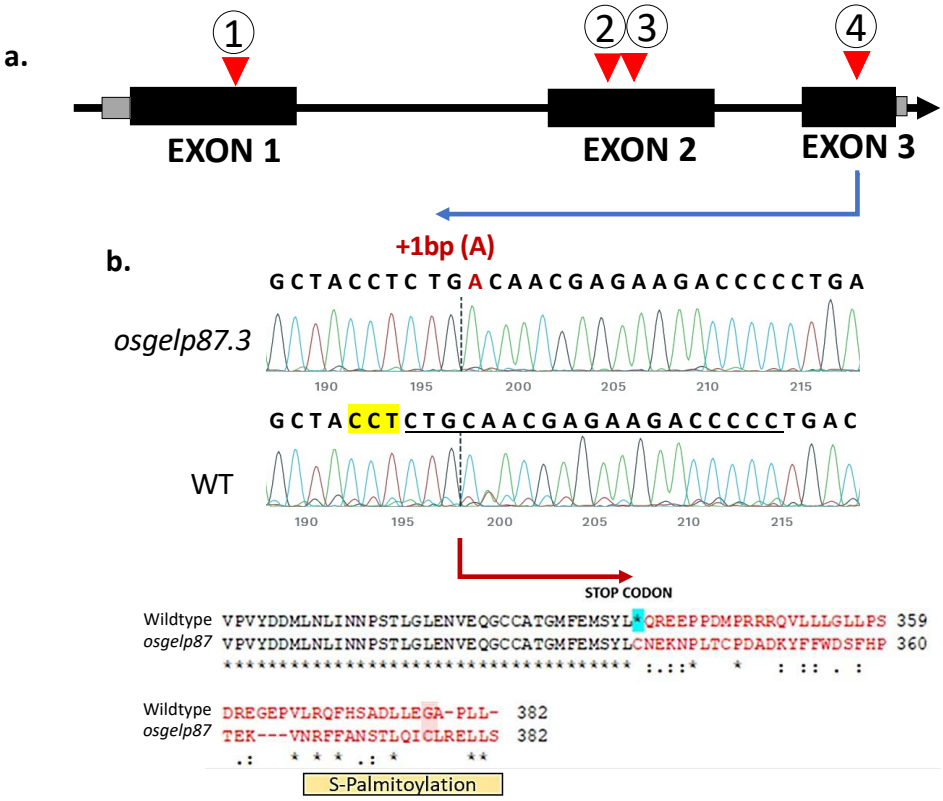

a.
1
2 3
4
EXON 1
EXON 2
EXON 3
b.
+1bp (A)
G C T A C C T C T G A C A A C G A G A A G A C C C C C T G A
osgelp87.3
190 195 200 205 210 215
G C T A C C T C T G C A A C G A G A A G A C C C C C T G A C
WT
190 195 200 205 210 215
STOP CODON
Wildtype VPVYDDMLNLINNPSTLGLENVEQGCCATGMFEMSYL*QREEPPDMPRRRQVLLLGLLPS 359
osgelp87 VPVYDDMLNLINNPSTLGLENVEQGCCATGMFEMSYLCNEKNPLTCPDADKYFFWDSFHP 360
Wildtype DREGEPVLRQFHSADLLEGA-PLL- 382
osgelp87 TEK---VNRFFANSTLQICLRELLS 382
S-Palmitoylation
c .
SP
α-19
α-20
SP
Wildtype (Nipponbare)
osgelp87-exon3 (in 1 bp A)

Fig. 3

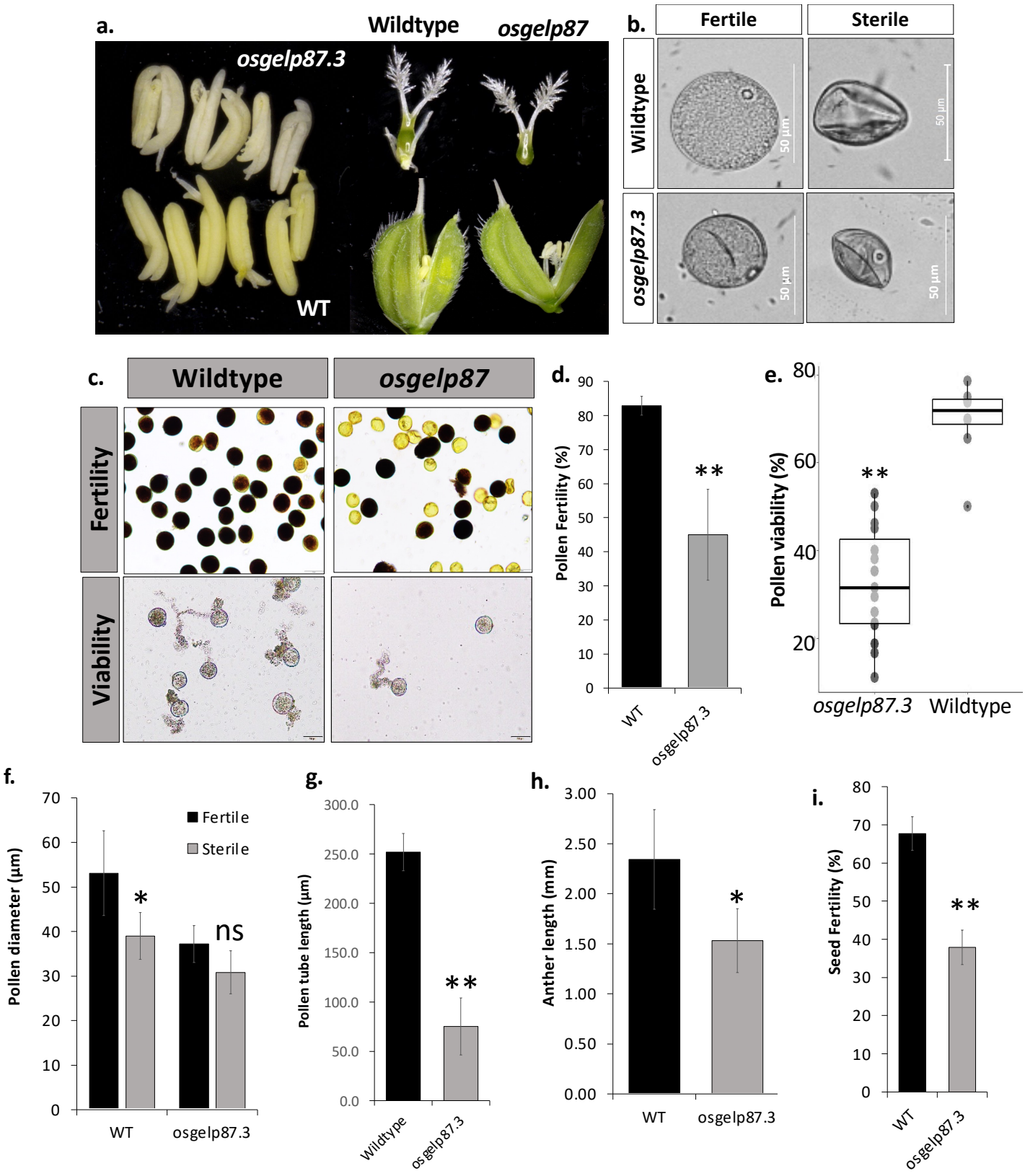

a.
Wildtype
osgelp87
osgelp87.3
WT
b.
Fertile
Sterile
Wildtype
osgelp87.3
50 µm
c.
Wildtype
osgelp87
Fertility
Viability
d.
Pollen Fertility (%)
**
WT
osgelp87.3
e.
Pollen viability (%)
**
osgelp87.3
Wildtype
f.
Pollen diameter (µm)
Fertile
Sterile
*
ns
WT
osgelp87.3
g.
Pollen tube length (µm)
**
Wildtype
osgelp87.3
h.
Anther length (mm)
*
WT
osgelp87.3
i.
Seed Fertility (%)
**
WT
osgelp87.3

Fig. 4

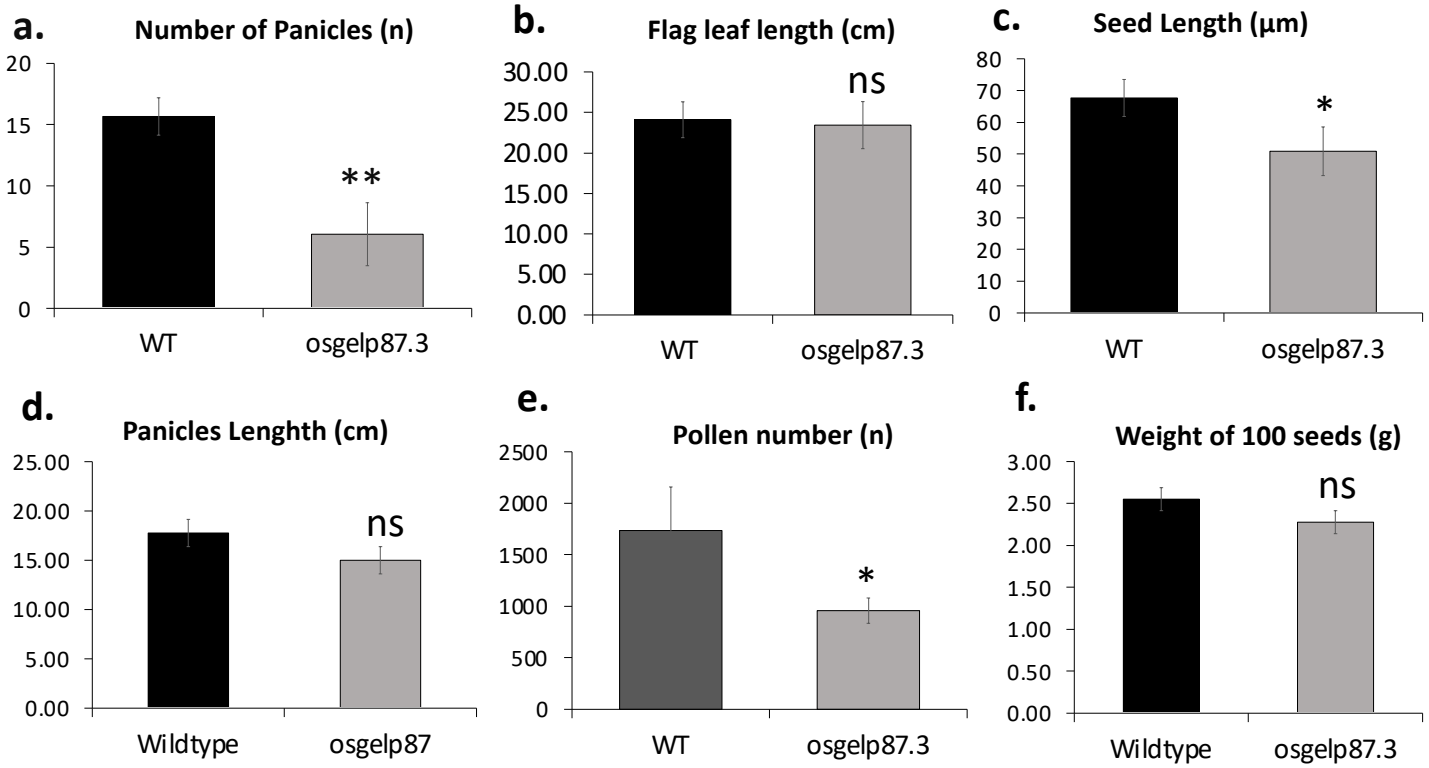
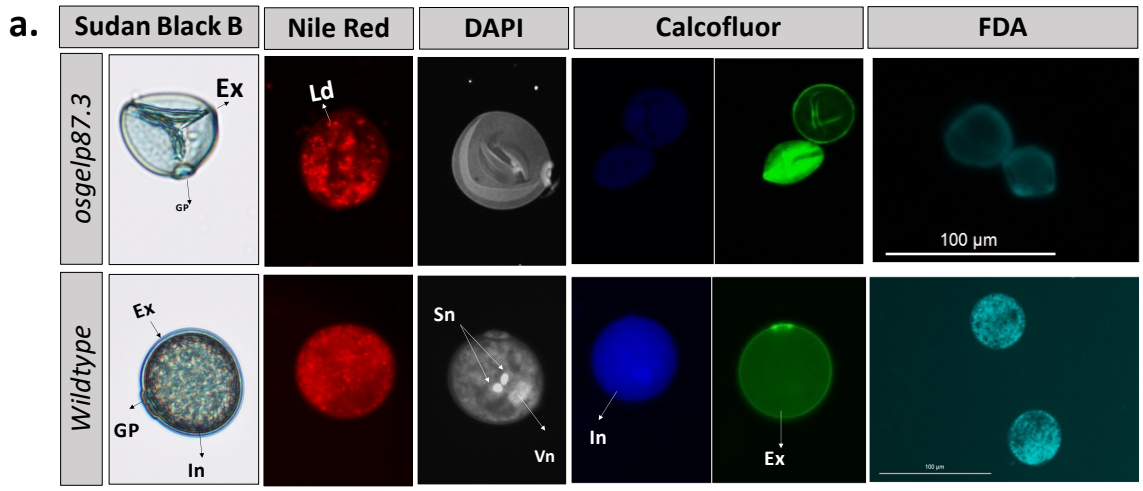
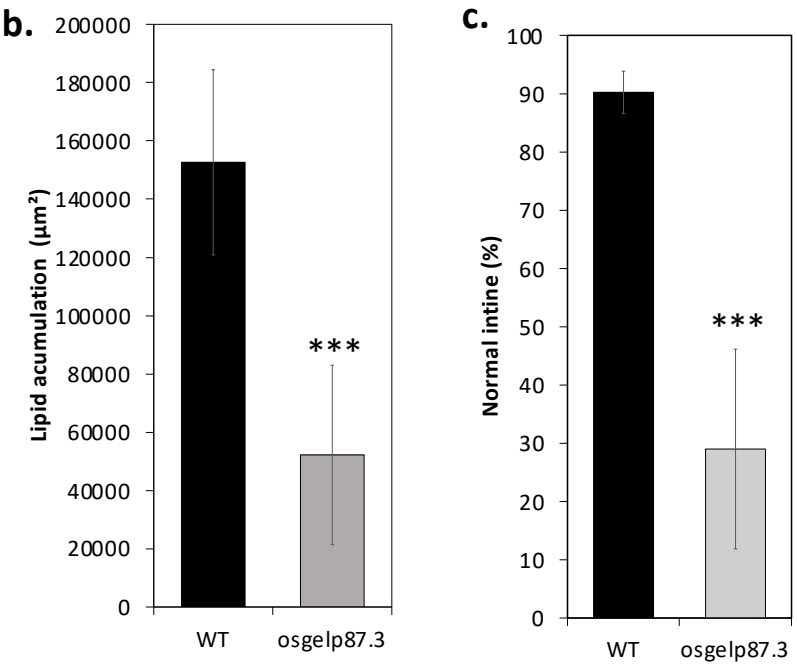

a.
Number of Panicles (n)
20
15
10
5
0
**
WT
osgelp87.3
b.
Flag leaf length (cm)
30.00
25.00
20.00
15.00
10.00
5.00
0.00
ns
WT
osgelp87.3
c.
Seed Length (µm)
80
70
60
50
40
30
20
10
0
*
WT
osgelp87.3
d.
Panicles Lenghth (cm)
25.00
20.00
15.00
10.00
5.00
0.00
ns
Wildtype
osgelp87
e.
Pollen number (n)
2500
2000
1500
1000
500
0
*
WT
osgelp87.3
f.
Weight of 100 seeds (g)
3.00
2.50
2.00
1.50
1.00
0.50
0.00
ns
Wildtype
osgelp87.3

Fig. 5


a.
Sudan Black B
Nile Red
DAPI
Calcofluor
FDA
osgelp87.3
Wildtype
Ex
GP
Ld
Sn
Vn
In
100 µm


b.
Lipid acumulation (µm²)
200000
180000
160000
140000
120000
100000
80000
60000
40000
20000
0
***
WT
osgelp87.3

c.
Normal intine (%)
100
90
80
70
60
50
40
30
20
10
0
***
WT
osgelp87.3

Fig. 6

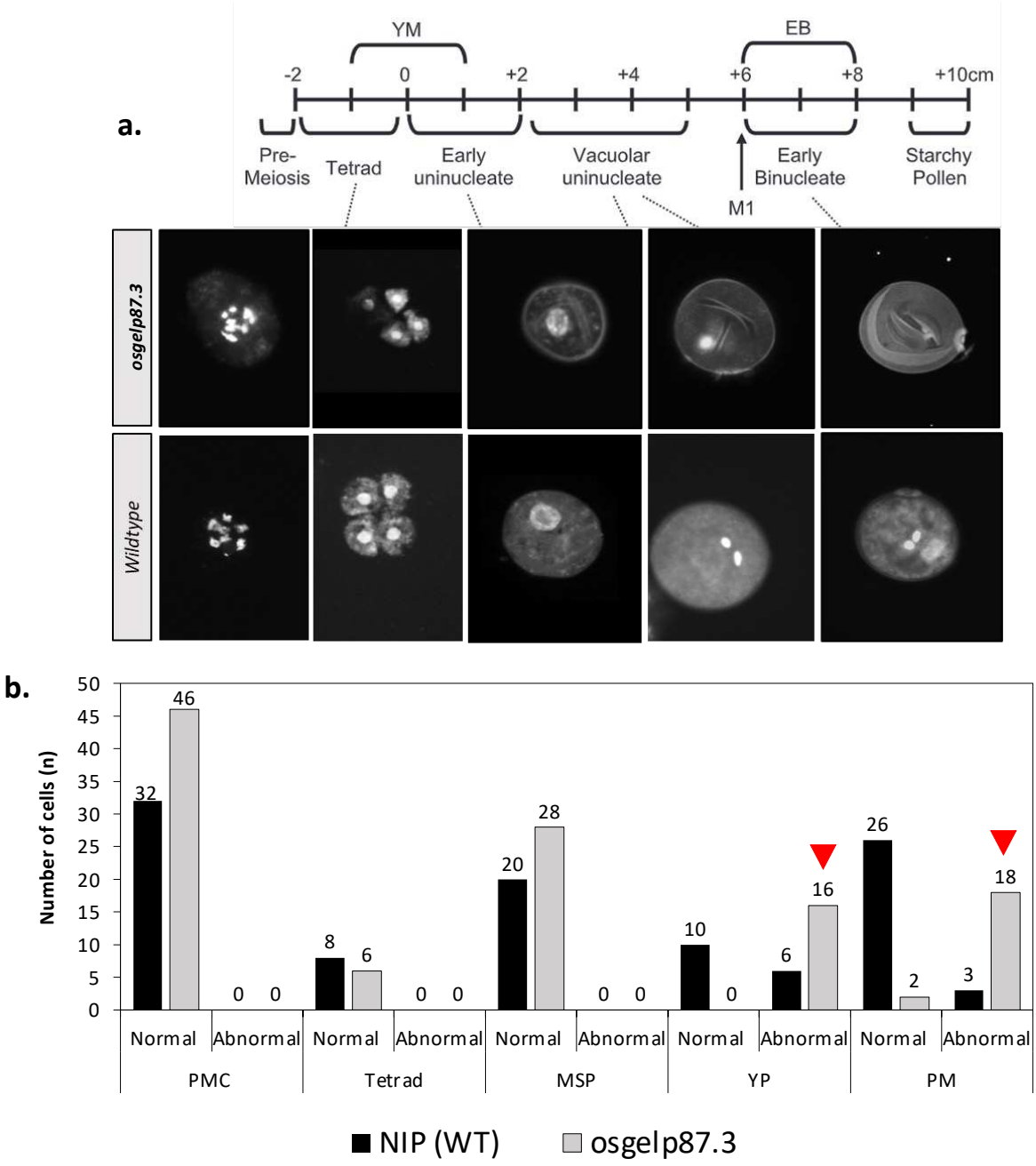

a.
YM
EB
-2
0
+2
+4
+6
+8
+10cm
Pre-Meiosis
Tetrad
Early uninucleate
Vacuolar uninucleate
M1
Early Binucleate
Starchy Pollen
osgelp87.3
Wildtype
b.
Number of cells (n)
50
45
40
35
30
25
20
15
10
5
0
32
46
0 0
8
6
0 0
20
28
0 0
10
0
6
16
26
2
3
18
Normal
Abnormal
Normal
Abnormal
Normal
Abnormal
Normal
Abnormal
Normal
Abnormal
PMC
Tetrad
MSP
YP
PM
NIP (WT)
osgelp87.3

Fig. 7

a.

No	ID Locus	Symbol	Annotation (RAP-DB)	A	LTP	Reference
Genes that are highly expressed in the wild type but UPREGULATED in the osgelp87 mutant						
1	*Os06g0133000*	*WX1*	Granule-bound starch synthase, Synthesis of amylose in endosperm			Lin et al., 2024
2	*Os02g0725500*	*OsENODL9*	early nodulin-like protein 9			Ma et al., 2011
3	*Os12g0420100*	*Os12BGlu38*	Beta-D-glucosidase 38			Shim et al., 2022
4	*Os04g0398700*	*PS1*	Similar to Pollen specific protein C13 precursor.			Lin et al., 2008; Cook and Thilmony, 2012
5	*Os08g0515900*	*DFR3*	Similar to Dihydroflavonol-4-reductase			Shih et al., 2008
6	*Os10g0465700*	*OsSTA246*	Beta-amylase 2			Ling et al., 2015
7	*Os05g0158600*	*GA2OX1*	Similar to OsGA2ox1			
8	*Os10g0548600*	*OsExPB9*	Beta-expansin precursor.			
9	*Os08g0326700*	*OsSub55*	Similar to subtilisin-like protease			
10	*Os03g0141200*	*OsBamy2*	Beta-amylase, Control of transient starch degradation			
11	*Os12g0115500*	*OsLTP1.20*	Similar to nonspecific lipid-transfer protein 3			
12	*Os11g0116000*	*OsLTP1.12*	Similar to Nonspecific lipid-transfer protein 1 (LTP 1)			
13	*Os11g0116200*	*OsLTP1.13*	Similar to nonspecific lipid-transfer protein 3.			
14	*Os01g0851700*	*Pho2*	Similar to Cytosolic starch phosphorylase			Ajmera et al., 2017
15	*Os04g0413200*	*OSINV4*	Cell-wall Invertase 3			Oliver et al., 2005
16	*Os11g0156200*	*OsProCP5*	Peptidase S28 family protein.			
17	*Os05g0543000*	*OSIPP3*	Pectin methylesterase inhibitor protein			Selvam et al., 2015
18	Os10g0351700	*MORE1C*	Glycosyl hydrolase family 10 protein, plant disease			
19	*Os06g0319133*	*OSJAGP*	Arabinogalactan protein homologue			
20	*Os05g0319800*	*OsHA1*	Similar to Plasma membrane H+ ATPase (EC 3.6.3.6))			
21	*Os01g0594500*	*OsTHI18*	Conserved hypothetical protein			
22	*Os01g0594900*	*OsTHI27*	Conserved hypothetical protein			
23	*Os01g0976200*	*OsCDP1.5*	11-S plant seed storage protein family protein			
Genes that are highly expressed in the wild type but DOWNREGULATED in the osgelp87 mutant						
1	*Os02g0626100*	*OsPAL_1*	Similar to Phenylalanine ammonia-lyase			
2	*Os12g0244100*	*HSP70_2*	Heat shock protein Hsp70 family protein			
3	*Os01g0600900*	*CAB2R*	Chlorophyll a-b binding protein 2, chloroplast precursor			
5	*Os01g0720500*	*Lhcb1.1*	Similar to Type I chlorophyll a/b-binding protein b			
7	*Os11g0582500*	*OSC6*	Protease inhibitor, lipid transfer protein (LTP), Postmeiotic anther development			Zhang et al., 2010
8	*Os11g0167800*	*OsASR5*	Abscisic acid-, stress-, and ripening-induced (ASR) protein			Li et al., 2017
9	*Os03g0808500*	*OsLTP1.3*	Plant lipid transfer protein/Par allergen family protein.			
10	*Os10g0148000*	*OsLTPd11/OsLTP6*	Lipid transfer protein, Drought tolerance			Liu et al., 2013
12	*Os08g0565900*	*OsGELP96*	Lipase, GDSL domain containing protein.			
13	*Os05g0477900*	*OsLTP1.4*	Similar to nonspecific lipid-transfer protein.			

: Anther specific gene
: Lipid transfer gene

b.

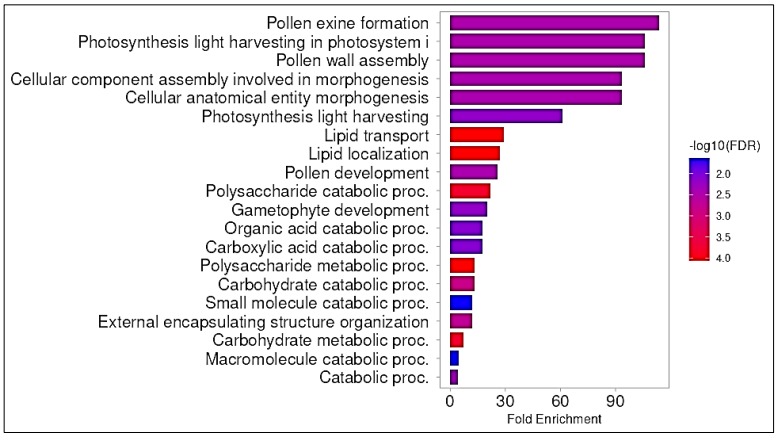


Fig. 8

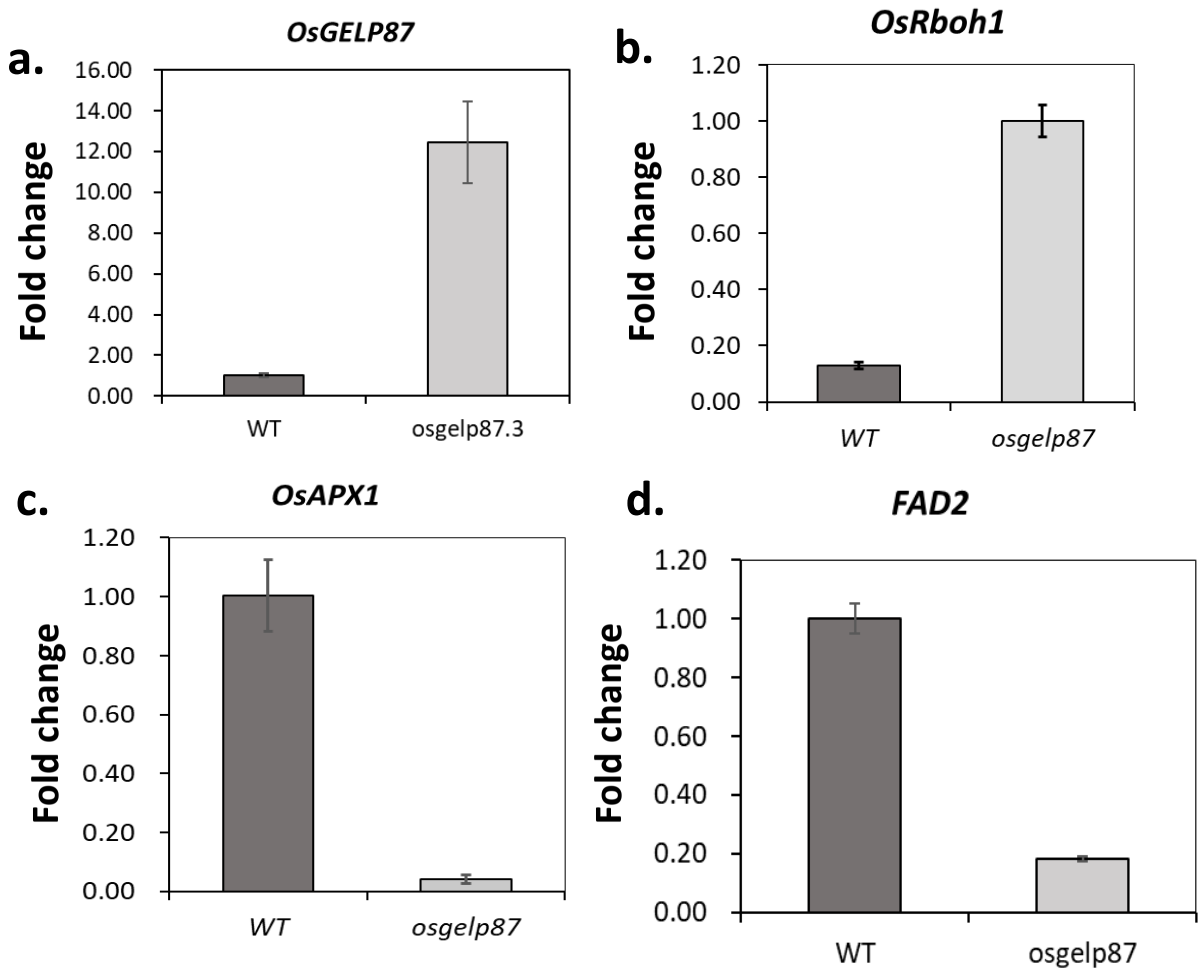

a.
OsGELP87
Fold change
16.00
14.00
12.00
10.00
8.00
6.00
4.00
2.00
0.00
WT
osgelp87.3
b.
OsRboh1
Fold change
1.20
1.00
0.80
0.60
0.40
0.20
0.00
WT
osgelp87
c.
OsAPX1
Fold change
1.20
1.00
0.80
0.60
0.40
0.20
0.00
WT
osgelp87
d.
FAD2
Fold change
1.20
1.00
0.80
0.60
0.40
0.20
0.00
WT
osgelp87

Fig. 9

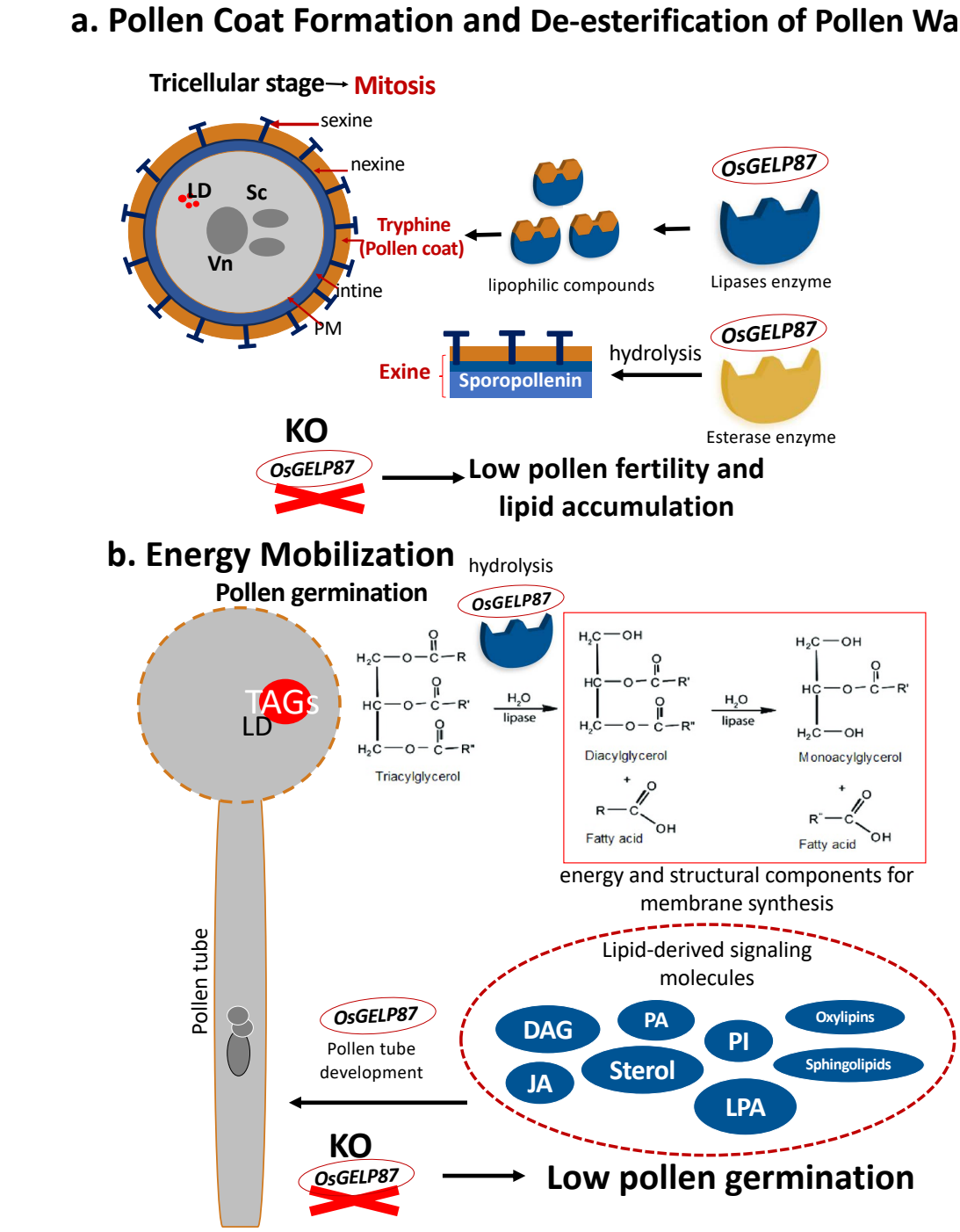
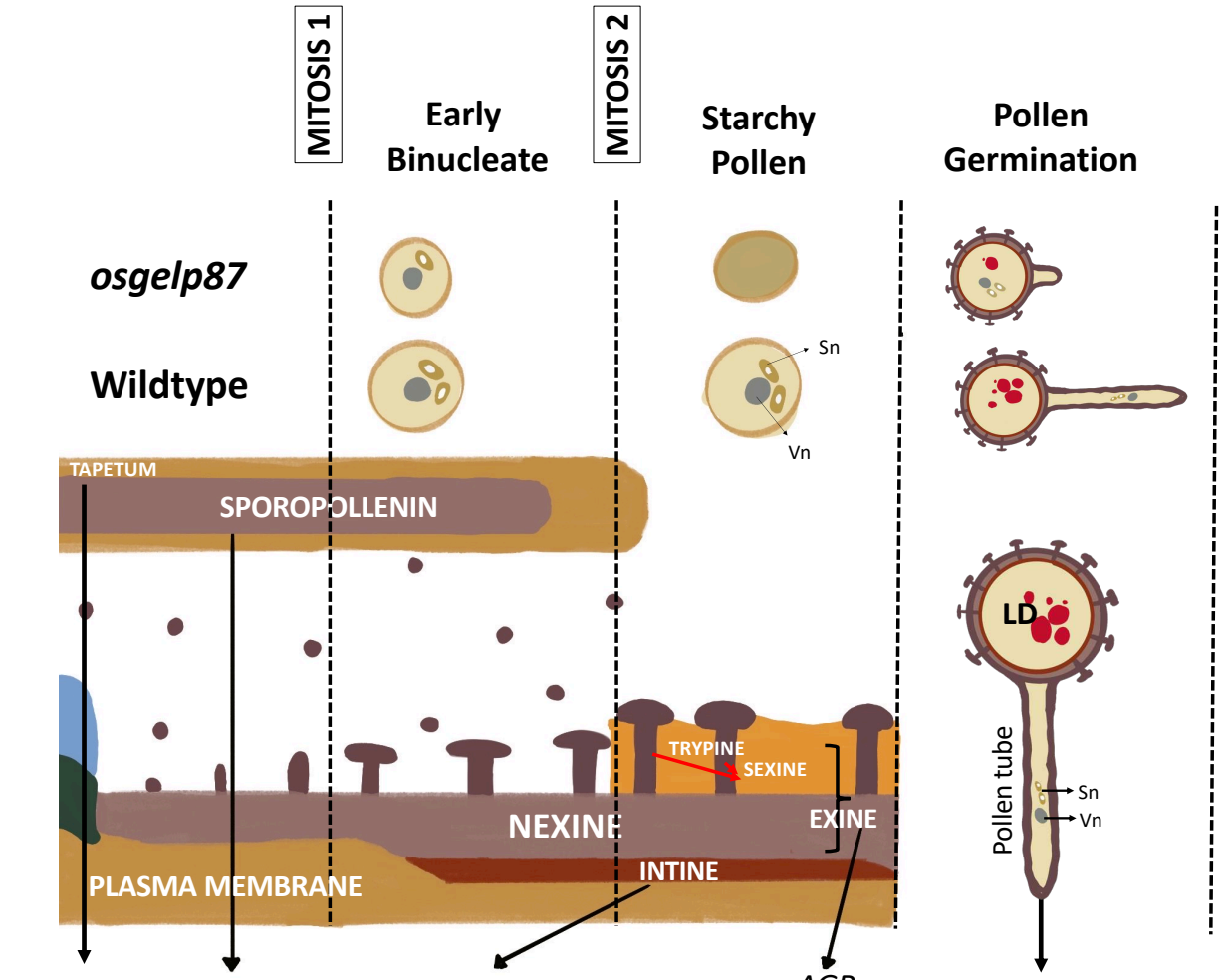

a. Pollen Coat Formation and De-esterification of Pollen Wall
Tricellular stage
Mitosis
sexine
nexine
LD
Sc
Vn
intine
PM
Tryphine
(Pollen coat)
lipophilic compounds
OsGELP87
Lipases enzyme
Exine
Sporopollenin
hydrolysis
OsGELP87
Esterase enzyme
KO
OsGELP87
Low pollen fertility and
lipid accumulation
b. Energy Mobilization
Pollen germination
hydrolysis
OsGELP87
TAGs
LD
Triacylglycerol
H2O
lipase
Diacylglycerol
H2O
lipase
Monoacylglycerol
Fatty acid
Fatty acid
energy and structural components for
membrane synthesis
Pollen tube
Lipid-derived signaling
molecules
DAG
PA
PI
Oxylipins
Sterol
Sphingolipids
JA
LPA
OsGELP87
Pollen tube
development
KO
OsGELP87
Low pollen germination

Fig. 10



AMS
BMI
DYTI
EAT1
GAMYB
MSP1
MS1
MS188
OSINV4
OsENODL9
OsLTP6

ACOS5
CYP703A2
CYP703A3
CYP704B1
DPW
MS2
OsC6
OsPAL1
OsDFR

CAP1
CESA
EFOP4&3
FLA3&14
MS6021
OsGT1
OsmiR528
OsGELP87

OsUCL23
Os12BGlu38
PMEs
RGP
RIP1
USP
MADS3
OsGT1

AGPs
MYB99
SEC23A/D
bZIP34
OsC6
OsGELP110/115
OsLTP1.20
OsLTP1.12
OsLTP1.13

OSIPP3
OsExPB9

Fig. 11

Supplementary Files

This is a list of supplementary files associated with this preprint. Click to download.

- Lubbaetal.SUPPLEMENTARYFIGUREManuscript2LB2026.03.09.pdf